Techno-economic optimization of utility-scale battery storage integration with a wind farm for wholesale energy arbitrage considering wind curtailment and battery degradation

Journal of Energy Storage 112 (2025) 115500

Contents lists available at ScienceDirect

Journal of Energy Storage

journal homepage: www.elsevier.com/locate/est

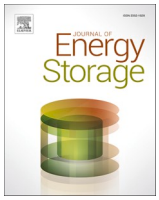

Research papers

Techno-economic optimization of utility-scale battery storage integration with a wind farm for wholesale energy arbitrage considering wind curtailment and battery degradation

Alberto Grimaldi [a,b,*], Francesco Demetrio Minuto [a,b], Alessandro Perol [c], Silvia Casagrande [c], Andrea Lanzini [a,b]

[a] Department of Energy, Politecnico di Torino, Corso Duca degli Abruzzi 24, 10129 Torino, Italy
[b] Energy Center Lab, Politecnico di Torino, Via Paolo Borsellino 38/16, 10138 Torino, Italy
[c] Edison S.p.A., Via Paolo Borsellino 38/16, 10138 Torino, Italy

ARTICLE INFO

Keywords:
Battery energy storage system
Wind-battery storage coupled system
Wholesale energy arbitrage service
MILP optimization
Wind curtailment
Battery degradation

ABSTRACT

Integrating energy storage into renewable generation systems offers significant potential for enhancing revenue streams. This study conducts a comprehensive long-term techno-economic analysis of integrating a battery energy storage system (BESS) with an existent wind farm for wholesale energy arbitrage and wind curtailment mitigation. The study identifies the optimal battery size and the corresponding optimal scheduling operations using a computationally efficient optimization framework formulated as a mixed-integer linear programming (MILP) problem. The MILP model maximizes net profit by considering real-world operational data, including wholesale electricity prices, wind generation, and transmission system operator dispatching orders from the Italian electricity market. Additionally, a cycle-counting battery degradation model is incorporated to account for the effects of battery ageing on the system performance. The study compares the financial performance of the wind-battery system with a scenario without storage, evaluating key energy, economic, and design indicators derived from the optimization results. Sensitivity analyses are performed, considering the most relevant key performance indicators, such as battery cost, battery efficiency, and wind curtailed energy. Results indicate that the highest net present value (NPV) of 152 k€ is achieved with a 1-h BESS of 4 MW / 4 MWh, while a 2-h BESS configuration with a size of 2 MW/4 MWh yields an NPV of 142 k€. The sensitivity analysis on battery capital expenditure cost reveals that for the integration of the battery into an existing wind farm to be financially viable, the battery cost must decrease below 325 €/kWh to achieve an interest rate of return (IRR) hurdle rate of 8–9 %. This work demonstrates the profitability potential of coupling BESS with wind farms and provides actionable insights for optimizing storage configurations in competitive electricity markets. Future work will expand the analysis to include ancillary services and uncertainty modeling further to enhance the economic and operational value of BESS integration.

Nomenclature

Abbreviations

BESS	battery energy storage system
CAPEX	capital expenditure
DAM	day-ahead market
DOD	depth of discharge

Variables

r	discount rate [%]
j	episode considered to evaluate the degradation coefficient [-]
$bigM$	bigM method constant
EOL	battery end of life [%]
$P_{gen}^{wind}(t)$	wind farm AC generated power [MW]
$EP(t)$	wholesale energy price [€/MWh]
$P_{ord}^{TSO}(t)$	TSO energy dispatching orders [MW]
$P_{grid}^{wind}(t)$	wind-to-grid power flow [MW]

(*continued on next column*)

(*continued*)

(*continued on next page*)

* Corresponding author at: DENERG, Politecnico di Torino, Corso Duca degli Abruzzi 24, 10129 Torino, Italy.
E-mail address: alberto_grimaldi@polito.it (A. Grimaldi).

https://doi.org/10.1016/j.est.2025.115500
Received 14 October 2024; Received in revised form 10 January 2025; Accepted 20 January 2025
Available online 26 January 2025

(*continued*)

EMS	energy management system	r_{p-e}^{bess}	BESS power-to-energy ratio [MW/MWh]	$P_{dh}^{bess}(t)$	BESS discharge power flow [MW]
GME	gestore dei mercati energetici	cf_{wind}	wind farm annual capacity factor [%/year]	$P_{ch-grid}^{bess}(t)$	grid-to-BESS charge power flow [MW]
MILP	mixed-integer linear programming	cf_{bess}	BESS annual capacity factor [%/year]	$P_{ch-wind}^{bess}(t)$	wind-to-BESS charge power flow [MW]
OPEX	operating expenditure	s_{curt}^{wind}	wind farm annual curtailed energy share [%/year]	$P_{loss}^{wind}(t)$	wind farm power losses flow [MW]
RES	renewable energy sources	s_{bess}^{wind}	wind-to-BESS share [%/year]	$P_{tot}^{bess}(t)$	sum between the BESS charge and discharge power flows [MW]
POD	point of delivery	s_{grid}^{wind}	wind-to-grid share [%/year]	$\mu_{deg,j}$	BESS degradation coefficient evaluated during episode j [€/MWh]
PUN	prezzo unico nazionale	*NPV*	net present value [€]	$E_{start,j}^{rem}$	BESS remaining capacity at the start point of the episode j [%]
RTM	real-time market	*LCOS*	levelized cost of storage [€/MWh]	$E_{end,j}^{rem}$	BESS remaining capacity at the end point of the episode j [%]
SCADA	supervisory control and data acquisition	*IRR*	interest rate of return [%]	$E_{rem,e}^{bess}(cyc)$	BESS remaining capacity function of the number of cycles [%]
SOC	state of charge	*PBT*	payback time period [years]	$SOC(t)$	BESS state of charge [MWh]
TSO	Transmission system operator	$\mathbb{R}_{exp}^{wind}$	wind farm export revenue [€]	$cyc_{rate}^{bess}(t)$	BESS fractional cycle rate in period t [-]
MILP-based power-energy model		$\mathbb{R}_{exp}^{bess}$	BESS export revenue [€]	$\beta_{dh}^{bess}(t)$	integer variable related to BESS discharge power flow [0, 1]
Sets and Index		$\mathbb{C}_{imp}^{bess}$	BESS import cost [€]	$\beta_{ch-grid}^{bess}(t)$	integer variable related to grid-to-BESS charge power flow [0, 1]
T	time scheduling period [h]	$\mathbb{C}_{cur}^{wind}$	wind farm curtailment cost [€]	$\beta_{ch-wind}^{bess}(t)$	integer variable related to wind-to-BESS charge power flow [0, 1]

(*continued on next column*)

(*continued*)

T_{roll}	rolling time scheduling period [h]	$\mathbb{C}_{deg}^{bess}$	BESS degradation penalty function [€]
t	index of the optimization time steps	$\mathbb{C}_{pen}^{bess}$	BESS penalty cost due to ageing [€/MWh]
Parameters and indicators		$\mathbb{C}_{capex}^{bess}$	BESS investment CAPEX cost [€]
Δt	time interval of the optimization problem [h]	$\mathbb{C}_{opex}^{bess}$	BESS OPEX cost [€]
E_{nom}^{bess}	BESS nominal capacity [MWh]	$\mathbb{R}_{cum}^{bess}$	BESS lifetime cumulative revenue [€]
P_{nom}^{bess}	BESS nominal power [MW]	$\mathbb{C}_{cum}^{bess}$	BESS lifetime cumulative cost [€]
P_{nom}^{wind}	wind farm nominal power [MW]	$E_{dh,tot}^{bess}$	total BESS energy discharged [MWh]
$\eta_{ch-wind}^{bess}$	BESS charge from wind efficiency [-]		
$\eta_{ch-grid}^{bess}$	BESS charge from grid efficiency [-]		
η_{dh}^{bess}	BESS discharge efficiency [-]		
η_{self}^{bess}	battery self-discharge losses [%/h]		

1. Introduction

In the modern electricity grids, characterized by a progressively increased share of intermittent renewable energy sources (RES), utility-scale battery energy storage systems (BESS) are considered a pivotal element to facilitate the massive RES integration due to their ability to smooth out the unpredictable RES power fluctuations. BESS has been found to be the most versatile energy storage technology due to its capability to provide multiple services to the electricity grid, ranging from energy-based services (e.g., energy arbitrage, load shifting), which helps to balance electricity supply and demand, to power-based services (e.g., ancillary services) which contribute to maintaining grid stability and security of supply.

As reported by the IEA World Energy Outlook Special Report on Batteries and Secure Energy Transitions [1], battery storage deployment in electricity markets has increased exponentially worldwide in recent years, from 1 GW in 2013 to over 85 GW in 2023. RES integration via energy shifting and the provision of peaking capacity are the primary applications of utility-scale batteries installed in recent years, especially in electricity systems with high shares of variable renewables with near-zero marginal costs [2,3]. When a BESS integrated with a renewable power plant participates in competitive electricity markets, it can capitalize on its energy shifting potential by participating in energy arbitrage, taking advantage of price spreads on wholesale electricity markets by charging during low-price periods and discharging during high-price periods. BESS can also support renewable energy curtailment by storing the excess energy during curtailment periods [4]. The BESS can not only profit through wholesale energy arbitrage but also make additional income by providing ancillary services to the power grid [5].

Among the different RES technologies, wind power has the largest share of generation and can participate in wholesale, e.g., day-ahead market (DAM) and real-time market (RTM) [6]. Integrating BESS in

wind farms may fulfill their production commitment in the DAM and buy/sell energy from/in RTM. [6]. The BESS is the most used energy storage technology to mitigate wind power fluctuation due to its easy implementation and small required installation area [7]. However, introducing BESS in wind farms will result in a considerable increase in capital costs. For this reason, an energy management system (EMS) control strategy is crucial to optimize the BESS's use and eventually reduce the capacity and investment of BESS [7].

1.1. Literature review

In the field of scientific research assessing the techno-economic performance of utility-scale renewable power plants combined with BESS, there are two primary methods for simulating resource dispatch and evaluating the value of energy generation assets: price-taker and price-maker modeling. Price-taker simulations focus on optimizing resource dispatch based on historical or predicted electricity prices, aiming to maximize the net revenue for the energy facility owner [8–13]. The key assumption in price-taker simulations is that the storage device is sufficiently small to have a marginal impact on electricity prices. On the other hand, price-maker models, also named production cost models, optimize the commitment and dispatch strategies across a fleet of energy generators to minimize the overall system costs of meeting electricity demand [14–19]. Since BESS capacities are usually small compared to conventional generation units participating in energy markets, numerous prior investigations have undertaken the formulation of price-taker models. Thus, the BESS impact on energy prices could be neglected [20]. In this work, the price-taker approach is implemented.

The three main approaches used in literature to model BESS operations in techno-economic analyses are the power-energy, voltage-current, and concentration-current models. As reported in [21], most works that estimate the economic benefit of the energy arbitrage provided by BESS employ a power-energy model: it is the simplest model of the battery, which is seen as an energy reservoir in which the energy is pumped to store and from which the energy is drawn to consume. Accordingly, as reported by the recent review of Yang et al. [22], the power-energy model is also called the generic model, and it is the most used model for BESS energy management: it monitors the change in the state of charge (SOC) of the BESS due to power flowing in or out of the battery. Therefore, the changes in battery state by intervals can be described as a time series with discrete values of SOC.

The battery degradation effects due to ageing, in particular decreasing capacity, increasing resistance, and safety implications, can significantly impact the economics of a BESS in power system applications [23]. Battery ageing consists of calendar and cycle ageing. The former reflects the battery's inherent degradation over time, mainly due to the battery operating temperature and the SOC level [24]. The latter occurs each time the battery is charged and discharged, and it is strongly influenced by the depth of discharge (DOD), the average SOC of each cycle, and the average cell temperature [22]. One of the key factors of battery degradation in system modeling is the battery storage capacity loss, known as capacity fade [25]. In the battery manufacturing industry, it is widely acknowledged that the end-of-life (EOL) criterion of a battery (e.g., lithium-ion or lead-acid batteries) is reached when its usable capacity falls below 80 % [26] or 70 % of its initial value, as suggested by Marques et al. [27]. Therefore, degradation cannot be neglected in energy management processes, especially for long-term analysis. Several studies combined a power-energy model with an empirical degradation model to estimate the BESS profitability for energy arbitrage [28–31]. Other works incorporate the degradation effect enforcing operational limits [9,30], or using energy throughput models [32]. Another widely used approach is the rainflow counting algorithm, used to count the battery cycles over the time horizon. As proposed in [33,34], through this counting method, the SOC profiles can be converted to equivalent cycles, and factor-based semi-empirical models are used to evaluate the battery degradation. In this work, it is considered a cycle-counting degradation model incorporated into the optimization model. This approach is more advanced than the energy throughout model [21]. It relies on the non-linear ageing occurring from battery cycling: cycles with smaller DoD contribute less than cycles into the degradation of the battery [35]. Each cycle with a certain depth-of-discharge is assigned with a fixed amount of degradation to the energy capacity according to the cycle depth ageing stress function that can be obtained from the experimental data.

As pointed out in [21,36,37], the deterministic mathematical optimization framework, and in particular the mixed-integer linear programming (MILP) approach, is one of the most widely used techniques to simulate the BESS operations when participating in competitive markets. In [12,38] the authors developed a MILP optimization model and a cycle-counting degradation model of a battery energy storage system providing energy arbitrage and operating reserve services. Similarly, in [20] a MILP optimization model is used to estimate the potential profit of a battery storage that provides energy arbitrage, operating reserve, and frequency regulation service participating in a competitive electricity market, but without considering the degradation effect due to battery ageing. One of the main limits of the above-mentioned works is that the battery capacity remains constant over the whole selected time horizon. Differently, in [39] the battery energy capacity degrades along the time horizon, and a MILP approach is used to simulate the optimal BESS dispatch operations considering the energy arbitrage, operating reserve, and frequency regulation service, but instead of cycle-counting degradation model, the degradation effect is evaluated by enforcing operational limits.

Considering wind-BESS modeling outcomes, several studies have investigated the integration of BESS with wind farms to enhance operational and economic performance in various market contexts. In [40] a detailed techno-economic optimization model was developed to evaluate the commercial viability of BESS integration for utilizing curtailed wind energy and replacing open and combined cycle gas turbine power plants in the UK electricity market. The economic model incorporated a simplified constant degradation approach, assuming an annual battery capacity reduction of 2 % over a 15-year lifespan, ultimately reaching an end-of-life capacity of 70 % relative to the initial value. Sheridan et al. [41] conducted an evaluation of co-located BESS and wind farms in the Irish electricity market, focusing on balancing market participation and wind curtailment reduction. However, their economic analysis relied on a simplified framework and was limited to short-term evaluations, lacking consideration of detailed operational dynamics and degradation effects over the full BESS lifespan. Feng et al. [42] developed a multi-objective three-level genetic algorithm (GA) for the optimal configuration of a PV-wind-BESS plant: the outer layer represented the model for determining the optimal BESS configuration, the middle layer focused on a multi-objective optimization model for BESS participation in electricity price arbitrage and reserve ancillary services operating in Zhejiang Province, China, and the inner layer coordinated the optimal scheduling of the PV-wind-BESS plant. Although their study incorporated multiple revenue streams, such as energy arbitrage and ancillary services, it excluded battery degradation modeling, a crucial factor for long-term economic analysis. Lobato et al. [43] assessed the economic viability of integrating BESS in a wind farm considering the Spanish electricity market. Three market applications have been examined (i.e., price arbitrage, balancing market, and wind schedule tracking) for different sizes of Li-ion and vanadium redox flow batteries integrated in a real Spanish 30 MW wind farm. Their findings indicate that in Spain, under the current regulatory framework, the viability of BESS depends largely on its participation in the balancing market, with profitability varying based on the system's size. Moreover, combining BESS usage across three different applications yields only marginal improvements in overall performance. To reduce the computational complexity of the optimization model, this study utilizes hourly-sampled data over weekly or monthly timeframes. Cremoncini et al. [44] explored hybrid energy

storage system (HESS) configurations in a study focused on a wind farm integrated with lithium-ion and redox flow batteries operating in the Danish market. Their analysis simulated energy arbitrage and automatic frequency restoration reserve (aFRR) using a robust optimization approach to address aFRR market uncertainties, alongside a MILP model for optimal dispatch. While their work examined the cyclic degradation of the lithium-ion battery, the techno-economic benefits of hybridization, the effects of robust optimization, and the influence of both constant and variable efficiencies, it did not include a long-term analysis covering the entire system lifespan, leaving gaps in understanding the cumulative economic impacts over time. Dicorato et al. [45] proposed a comprehensive procedure for planning and operating BESS in conjunction with wind farms within the Italian electricity market. The study employed a dynamic programming (DP) algorithm to optimize the energy dispatch of the combined wind-storage system, aligning generation forecasts with battery characteristics. Additionally, an economic feasibility analysis was conducted to evaluate the profitability of the wind-BESS integration. However, the study did not account for battery degradation or the mitigation of wind curtailment. Li et al. [46] investigated the operation of a co-located wind-BESS system in the Australian electricity market, utilizing a deep reinforcement learning (DRL) approach to maximize revenue from the spot market. Their study highlighted the BESS's dual potential in mitigating wind curtailment and performing energy arbitrage, demonstrating that previously curtailed wind energy could serve as an effective power source for charging the BESS, thereby generating additional financial returns. However, the analysis did not extend to a long-term techno-economic evaluation. Similarly, Khalid et al. [47], developed a model predictive control (MPC) strategy coupled with a DP tool to maximize the profit of a wind-BESS system while providing energy arbitrage service in the Australian electricity market. However, some key economic factors are not considered, such as operation and maintenance costs and battery degradation. Moghaddam et al. [6] investigated the profitability of a BESS co-located with a wind farm participating in the day-ahead (DA) and real-time (RT) markets within the midcontinent independent system operator (MISO) region in the U.S. The study began by determining the optimal BESS size using one year of historical wind power and electricity price data from MISO. Subsequently, a receding horizon control (RHC) scheme was developed, leveraging forecasted data generated by an autoregressive integrated moving average (ARIMA) model. Finally, the profitability of the BESS was assessed, incorporating the effects of voltage control, BESS lifetime, and battery price on average daily profits. However, the study did not include a long-term techno-economic assessment. Table 1 provides a summary of the literature survey on wind-BESS modeling approaches in techno-economic studies. A key observation from the studies reviewed is that the profitability of BESS participation in electricity markets varies significantly depending on the specific characteristics and regulations of the electricity market in question [48].

1.2. Aim and novelty of the study

The economic energy arbitrage potential of wind-battery systems has been widely studied in the literature. However, significant gaps remain in terms of modeling approaches, operational strategies, and economic assessments. As pointed out in [40], many existing works related to BESS providing energy-based applications primarily focus on alternative battery chemistries other than Li-ion (e.g., sodium-sulfur, vanadium-redox flow batteries), small-scale applications (e.g., kW to MW range), and technical suitability rather than economic viability. For instance, previous studies have explored the integration of BESS for industrial [49] or standalone applications [50], peak demand management in regional grids [51], or in commercial buildings [52]. While these studies provide valuable insights, they often neglect critical factors such as battery degradation, real-time dispatch optimization, and market-specific conditions, which are essential for assessing long-term financial viability. Additionally, the analysis of the existing literature has revealed that only a few studies are focused on MILP-based optimization techniques applied to multi-MW wind-battery systems participating in the Italian electricity market. Regarding the time horizon, as pointed out in [32], MILP-based simulations typically consider short periods (e.g., 1 year of operations) due to computational constraints. In contrast, this work simulates the entire 15-year lifetime of the BESS using the MILP-based power-energy model, providing more realistic results. Another limitation found in the existing literature is that the input data of the optimization models are typically predicted and/or assumed. On the contrary, in this work, the input data of the MILP-based optimization model are real data provided by the supervisory control and data acquisition (SCADA) of a commercial wind farm currently in operation in the Italian electricity market. A further aspect that distinguishes this work is its focus on wind curtailment mitigation, a factor rarely addressed in the literature. By evaluating the dual benefits of energy arbitrage and wind curtailment reduction, this study provides a comprehensive perspective on the economic and operational advantages of BESS integration. To better highlight the gaps in the current literature and emphasize the contributions of this study, the key limitations of existing works are summarized as follows:

- techno-economic analyses often consider only short-term operations (e.g., one year), failing to capture the full economic and operational impacts of long-term battery degradation.
- simplistic modeling frameworks, such as deterministic rule-based or heuristic approaches, are commonly used, which may not accurately reflect real market dynamics compared to robust MILP-based optimization frameworks.
- many studies rely on simplified constant degradation models or energy throughput models, neglecting the non-linear degradation effects tied to depth-of-discharge (DOD) and cycle-based battery ageing.
- several studies assume constant battery capacity over the entire simulation horizon, overlooking the progressive degradation effects that significantly impact long-term performance and profitability.

The present work expands on previous literature by developing a novel MILP-based optimization model applied to a wind-BESS system operative in the Italian electricity market while providing energy arbitrage as an energy-based service. Additionally, a cycle-counting degradation model based upon a semi-empirical degradation function is incorporated into the optimization model. The objective function of the MILP problem is a cost function that includes the revenue from energy arbitrage, the import cost due to battery charge from the grid, the degradation penalty function due to battery ageing, and the wind curtailment cost. Based on the optimal dispatch profiles obtained by the MILP model, a long-term profitability analysis is proposed during the entire system lifetime, considering the battery EOL criterion when its capacity reaches 70 % of its original capacity. In the proposed case study, the wind power production and dispatching order profiles data are taken from historical data of a wind farm currently in operation in the Italian electricity market. Historical wholesale electricity price data used for the energy arbitrage service are taken from the Italian electricity market.

To address the identified gaps, the present study aims to:

- Develop a robust and easily replicable optimization model to maximize the net profit derived by energy arbitrage by optimizing the wind-battery dispatch operations in the Italian electricity market, considering as time horizon the entire 15-year lifetime of the BESS.
- Evaluate the optimal design, energy, and economic indicators by conducting a long-term techno-economic analysis, considering the Italian electricity market as an applicative case.
- Offer guidelines for readers and power plant owners on how it is possible to incorporate a cycle-counting degradation model and wind

Table 1
Literature survey on wind-BESS models in techno-economic studies.

Study	System layout	Optimization framework	Wind-farm data source	Simulation horizon	Battery degradation model	Wind curtailment mitigation	Electricity market application	Electricity market location
[40]	Wind-BESS	LP[a] model for BESS size	UK National Grid	1 year	Constant annual decline	Yes	Grid-level peak demand management	UK
[41]	Wind-BESS	MATLAB Simulink	Electricity Supplier Board	1 year	Rainflow + empirical model	Yes	Balancing market and system services	Ireland
[42]	PV-wind-BESS	Multi-objective three-level GA[b]	Zhejiang Regulatory Office of National Energy Administration	1 year	Not considered	No	Energy arbitrage and reserve ancillary services	China
[43]	Wind-BESS	Deterministic rule-based	Real wind farm in Spain	Weekly/monthly profiles	SOC and efficiency dependence	No	Energy arbitrage, balancing market, and wind schedule tracking	Spain
[44]	Wind-HESS[C]	Robust optimization for uncertainty and MILP[d] for dispatch	Real wind farm in Denmark	1 year	Rainflow + DOD dependence	No	Energy arbitrage and automatic frequency restoration reserve	Denmark
[45]	Wind-BESS	DP[e]	Real wind farm in Italy	1 year	Not considered	No	Market-based delivery plan	Italy
[46]	Wind-BESS	DRL[f]	Real wind farm in Australia	1 year	Linear approximation using a specific battery cost-coefficient	Yes	AEMO[g] spot market: wind curtailment mitigation and energy arbitrage	Australia
[47]	Wind-BESS	MPC[h] for prediction and DP for dispatch	Real wind farm in Australia	1 day	Not considered	No	AEMO spot market	Australia
[6]	Wind-BESS	RHC[i] scheme for uncertainty and ARIMA[j] model for forecast	MISO[k]	1 year	Linear approximation per cycle	Yes	Day-ahead and real-time markets	U.S.
This work	Wind-BESS	MILP	Real wind farm in Italy	15 years	Cycle-counting with semi-empirical degradation curve	Yes	Energy arbitrage	Italy

[a] LP: Linear programming.
[b] GA: Genetic algorithm.
[C] HESS: Hybrid energy storage system.
[d] MILP: Mixed-integer linear programming.
[e] DP: Dynamic programming.
[f] DRL: Deep reinforcement learning.
[g] AEMO: Australian energy market operator.
[h] MPC: Model predictive control.
[i] RHC: Receding horizon control.
[j] ARIMA: Auto-regressive integrated moving average.
[k] MISO: Midcontinent independent system operator.

curtailment mitigation into the optimization model, enabling realistic profitability evaluations.

This work is organized as follows. In Section 2 it is presented the wind-BESS layout. Section 3 describes the methodology implemented to build the MILP optimization model, including the cycle-counting degradation model. Section 4 provides a comprehensive discussion of the results obtained by the proposed energy arbitrage service case study. Finally, conclusions and foreseen next steps are included in Section 5.

2. Wind-battery energy storage system layout

The system under investigation proposed in this work is a utility-scale wind-battery system that provides wholesale energy arbitrage service to the electricity grid. In Fig. 1 it is presented a schematic layout of the different components with the correspondent power flow pathways. The MW-scale wind farm, currently operative in the Italian energy market, is composed of several wind turbines connected to the AC electricity bus bar through a DC/AC inverter. Starting from the left, the three power flows of the wind farm (blue rows) are the wind power losses due to curtailment, the power generated by the wind farm directly sent to the grid, and the power generated by the wind farm to charge the battery. The proposed case study introduces a Li-ion battery energy storage system (BESS), which is AC-coupled with the wind farm. The AC-coupling architecture is chosen instead of the DC-coupling because utility-scale systems have relied primarily on AC-coupled architectures due to their enhanced flexibility because of a lack of affordable integrated hardware for DC-coupled systems [53]. The BESS is composed of the battery bank and the bidirectional inverter: the AC/DC rectifier for the battery charging process and the DC/AC inverter for the battery discharging process. It is assumed the same DC/AC efficiency of the rectifier to charge the battery from the wind farm or from the grid. The BESS discharging process is considered independent of the wind farm generation. The model allows for the configuration of two distinct values for charge and discharge efficiency. However, for the sake of simplicity, it is assumed a symmetric efficiency behavior between the battery charging and discharging process. Therefore, the battery charging efficiency is assumed to be equal to the battery discharging efficiency. Finally, the AC power flows are exchanged through the electricity grid at the point of delivery (POD) via a smart energy meter, and the wholesale energy arbitrage is simulated. The basic principle of this energy-based service consists of purchasing energy from t, the grid in low-price periods and selling it back to the grid during high-price periods on the energy wholesale market. The dispatching operations of the wind-battery system are managed by the proposed scheduling energy management system (EMS) model, based on a computationally efficient optimization logic formulated as a MILP problem. A more comprehensive description of the methodology used to build the MILP optimization model is presented in Section 3. The key assumptions and parameters of the wind-battery system used in this work are summarized in Table 2.

The input historical data are the hourly wind speed, the hourly electricity prices, and the hourly dispatching orders sent by the transmission system operator (TSO) operating in the Italian wholesale energy market. The wind speed and the dispatching orders data are extracted during the selected observation periods from the local supervisory control and data acquisition (SCADA) system of the wind farm. For each wind turbine of the wind farm, the AC wind power production is evaluated as a function of the wind speed according to the power curve of the wind turbines. As a result, the total AC power production of the wind farm is obtained by summing the AC power production of each wind turbine. In conclusion, electricity price data correspond to the Italian wholesale day-ahead market (DAM) energy price (Prezzo Unico Nazionale, PUN) sourced from GME for Italy (GME – Gestore dei Mercati Energetici S.p.A. [54]). Before selecting the 2023 price, different years

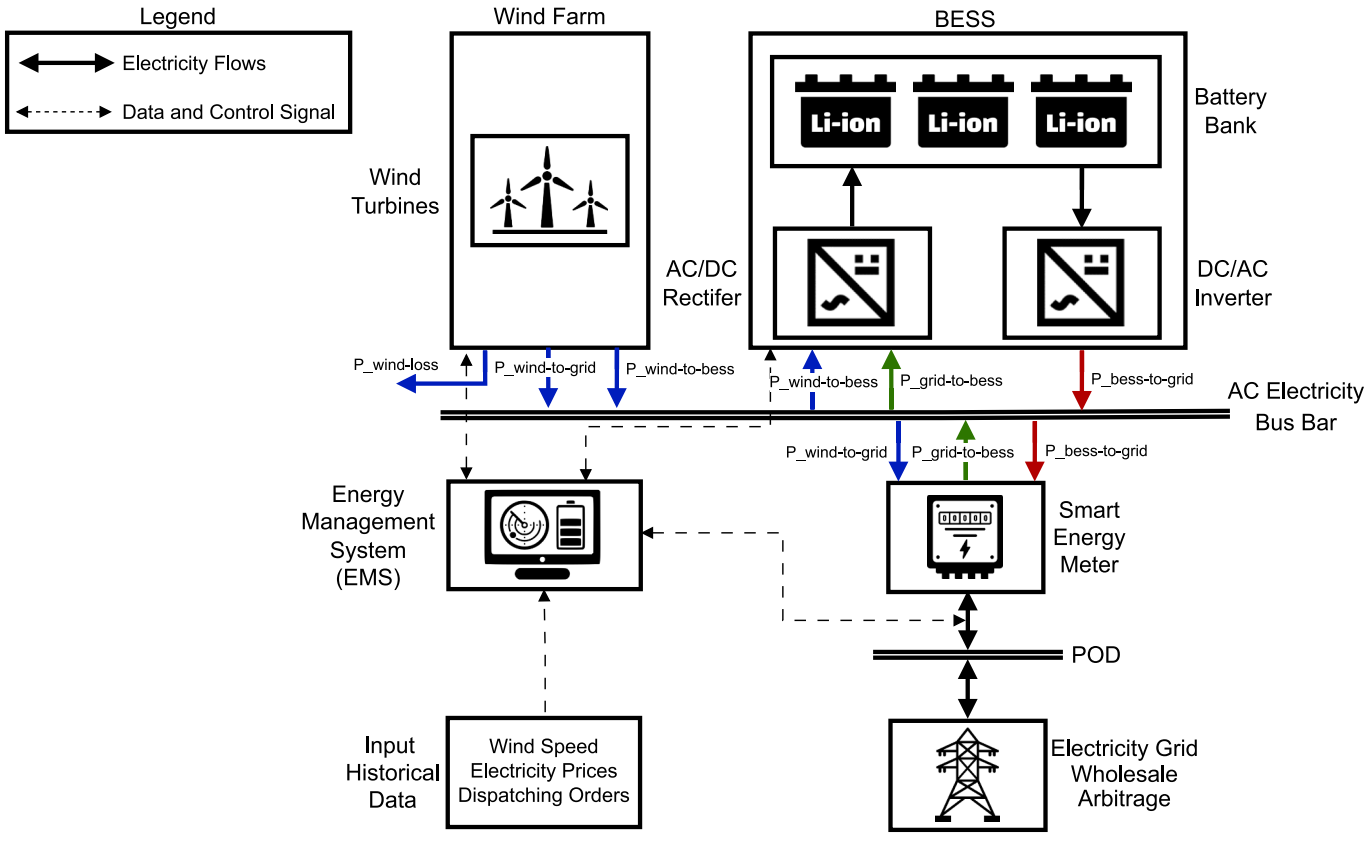

Fig. 1. Utility-scale wind-battery storage system layout.

Table 2
Main assumptions used for the MILP-based wind-battery modeling.

BESS parameters		Wind farm parameters[a]	
Storage type	NMC Lithium-ion	Nominal energy produced	≈90,000 MWh/year
EOL [27]	70 % - 6147 cycles	Average capacity factor	≈26.2 %/year
DC/AC rectifier efficiency (charging from wind farm) [55]	90 %	Curtailed energy	≈2000 MWh/year
DC/AC rectifier efficiency (charging from grid) [55]	90 %	Average curtailed energy ratio	≈2.2 %/year
AC/DC inverter efficiency (discharging to grid) [55]	90 %		
SOC range [56]	20 % - remaining capacity		
Self-discharge losses [56]	99.99 %/h		

[a] The historical time series raw data of the utility-scale wind farm used in this work is confidential.

were investigated. It was found that the 2023 electricity prices data can be considered as a business-as-usual scenario, hence a representative year.

3. Methodology

This section describes the methodology implemented to build the wind-battery MILP optimization model. The problem of finding the most profitable operational strategy for wholesale energy arbitrage service can be treated as an optimization problem [56]. The MILP optimization model implemented in this work is based upon the assumption that the wind-battery plant owner has perfect foresight of wind power production, electricity prices, and dispatching order profiles. Moreover, it is assumed that the utility-scale wind-battery system trades in the wholesale energy market, which provides the best financial opportunity for energy arbitrage service due to its high volatility.

The MILP model was built using the *pyomo*® optimization framework [57]. The toll was implemented in *Python*®, and the MILP optimization problem was solved using the *Gurobi*™ solver [58]. The time resolution used in the Python-based MILP model is $\Delta t = 1$ $[h]$, which is the same as the time resolution of the input historical data. As illustrated in Fig. 2, the proposed EMS optimal scheduling is based on a $T = 48$ $[h]$ time scheduling period. However, only the results of the first $T_{roll} = 24$ $[h]$ rolling time period are stored and transferred to the next scheduling period. This rolling time window technique is implemented to account for operations beyond the scheduling period and inter-temporal constraints in energy storage level that will affect operations in the next periods [32]. This optimal scheduling set-up is repeated over the BESS project lifetime considered in this work (i.e., $T_{BESS} = 15$ $[years]$).

The overall structure of the proposed methodology is presented in Fig. 3. The objective function of the optimization problem is to satisfy the TSO dispatching orders for each time step Δt of the optimization time horizon T while maximizing the net profit of the wind-battery system considering the wholesale energy arbitrage grid service. The input data to the MILP-based optimization process are the following:

i. Wind speed data converted into AC wind farm power production $\forall t \in T$.
ii. Wholesale energy prices data $\forall t \in T$.
iii. TSO energy dispatching orders $\forall t \in T$.
iv. Technical specifications of the wind-battery system.
v. BESS degradation curve, hence, the battery remaining capacity as a function of the battery number of cycles assuming an end-of-life (EOL) criterion of 70 % with respect to the nominal battery capacity.

The MILP-based optimization process returns the following decision variables:

i. The optimal scheduling operations of the wind-battery system, namely, the wind farm power production directly sent to the grid, the wind farm power production sent to charge the battery, the battery discharge power to the grid, the grid power sent to charge the battery, the wind farm power losses, and the battery SOC level $\forall t \in T$.
ii. Since the processes related to the battery charge from the wind farm, the battery charge from the grid, and the battery discharge to the grid cannot occur simultaneously, three integer variables associated with the correspondent continuous variables are obtained as the output of the MILP-based optimization model $\forall t \in T$.

Consequently, a post-processing elaboration (green box) is conducted based on the output (i.e., decision variables) of the optimization process. The goal is to perform a long-term tecno-economic analysis considering an applicative case in the Italian wholesale energy market

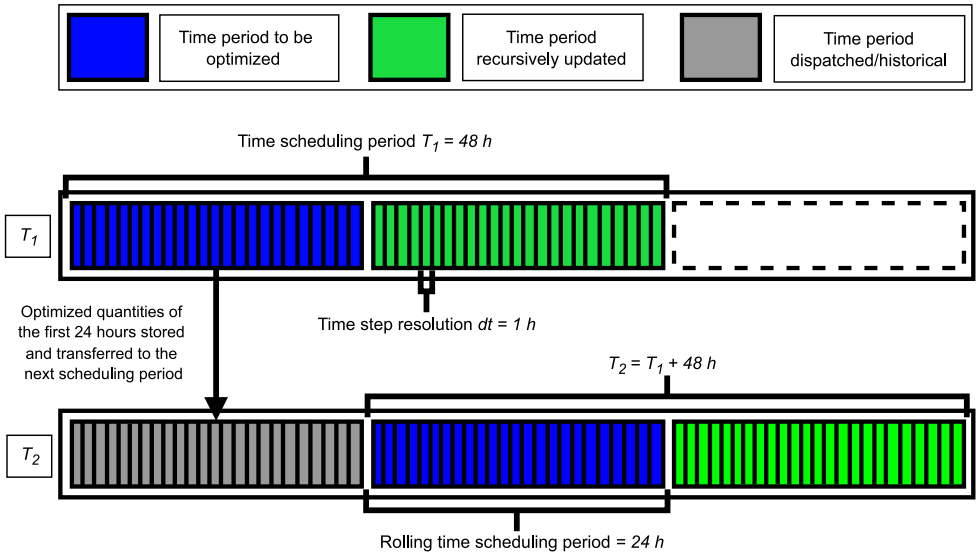

Fig. 2. Schematic diagram of the MILP optimization dispatch technique implemented in the wind-battery wholesale energy arbitrage model based upon a $T = 48$ $[h]$ time scheduling period and a $T_{roll} = 24$ $[h]$ rolling time period with a $\Delta t = 1$ $[h]$ resolution.

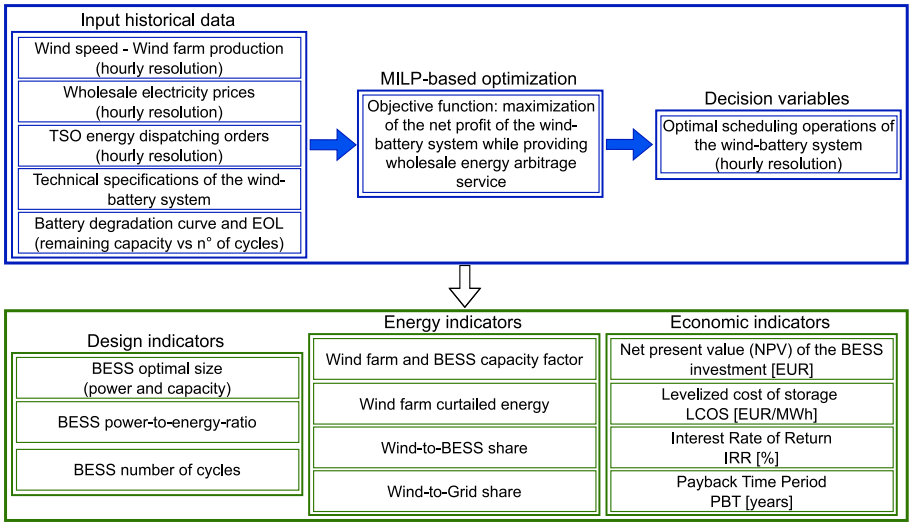

Fig. 3. Schematic layout of the methodology: optimization framework for the optimal design of the wind-battery system (blue box), post-processing framework for the evaluation of the most relevant key performance indicators (green box).

by evaluating the most relevant KPIs in terms of design, energy, and economic indicators.

3.1. Objective function

As defined in Eq. (1), the objective function of the MILP-based optimization problem corresponds to the maximization of the net profit $\mathbb{P}$ by netting the revenues and the costs resulting from the wholesale energy arbitrage service of the wind-battery system over its lifetime ($T_{BESS} = 15\ [years]$). More specifically, the overall net profit is the algebraic sum of the revenue obtained by exporting energy from the wind farm to the grid $\mathbb{R}_{exp}^{wind}$, the revenue obtained by exporting energy from the battery to the grid $\mathbb{R}_{exp}^{bess}$, the import cost due to importing energy from the grid to the battery $\mathbb{C}_{imp}^{bess}$, the wind farm curtailment cost due to the wind power losses $\mathbb{C}_{cur}^{wind}$, and the degradation penalty function due to battery ageing $\mathbb{C}_{deg}^{bess}$. The cost components are considered with a minus sign since the goal of the optimization problem is to minimize them, while maximizing the revenue components.

$$\begin{aligned} max\{\text{obj}\} &= max\left\{\sum_{t=1}^{T_{BESS}} \mathbb{P}\right\} \\ &= max\left\{\sum_{t=1}^{T_{BESS}} \mathbb{R}_{exp}^{wind} + \mathbb{R}_{exp}^{bess} - \mathbb{C}_{imp}^{bess} - \mathbb{C}_{cur}^{wind} - \mathbb{C}_{deg}^{bess}\right\} \end{aligned} \tag{1}$$

As reported in Eq. (2), the wind farm revenue component is evaluated by multiplying the wholesale energy price $EP(t)$ with the wind-to-grid power flow $P_{grid}^{wind}(t)$ for each time step Δt. Similarly, the BESS revenue component expressed in Eq. (3), is equal to the wholesale energy price multiplied by the BESS discharge power flow $P_{dh}^{bess}(t)$ for each time step Δt.

$$\mathbb{R}_{exp}^{wind} = \sum_{t=1}^{T_{BESS}} EP(t) \cdot P_{grid}^{wind}(t) \cdot \Delta t \forall t \in T\ [€] \tag{2}$$

$$\mathbb{R}_{exp}^{bess} = \sum_{t=1}^{T_{BESS}} EP(t) \cdot P_{dh}^{bess}(t) \cdot \Delta t \forall t \in T\ [€] \tag{3}$$

Considering now the cost components, the BESS import cost in Eq. (4) is equal to the wholesale energy price multiplied by the BESS charge flow from the grid $P_{ch-grid}^{bess}(t)$ for each time step Δt. The wind farm curtailment cost expressed in Eq. (5) is obtained by multiplying the wholesale energy price with the wind farm power loss flow $P_{loss}^{wind}(t)$ for each time step Δt. The wind curtailment cost represents the cost of energy that cannot be sold to the grid due to the presence of dispatch orders or stored in the battery when it is fully charged. This cost is included in the objective function with a negative sign to ensure that minimizing the curtailment cost simultaneously reduces the power losses from the wind farm caused by curtailment.

$$\mathbb{C}_{imp}^{bess} = \sum_{t=1}^{T_{BESS}} EP(t) \cdot P_{ch-grid}^{bess}(t) \cdot \Delta t \forall t \in T\ [€] \tag{4}$$

$$\mathbb{C}_{cur}^{wind} = \sum_{t=1}^{T_{BESS}} EP(t) \cdot P_{loss}^{wind}(t) \cdot \Delta t \forall t \in T\ [€] \tag{5}$$

The degradation penalty function due to battery ageing, reported by Eq. (6), is defined as the sum between the battery charge and discharge power flows at each time step, multiplied by the degradation coefficient $\mu_{deg,j}$. As defined in Eq. (7), the degradation coefficient represents the slope of the linear approximation of battery ageing, evaluated after each *j-th* episode. The time period of every *j-th* episode corresponds to the optimization time horizon $T = 48\ [h]$. The numerator of the degradation coefficient is the difference between the BESS remaining capacity at the start $E_{start,j}^{rem}$ and at the end $E_{end,j}^{rem}$ of the *j-th* time window. Since these components are defined as a percentage of the initial battery capacity, they are converted into energy terms by multiplying with the BESS nominal capacity E_{nom}^{bess} and dividing by 100. As defined by Eq. (8), the denominator of the degradation coefficient is the sum between the BESS charge and discharge power flows $P_{tot}^{bess}(t)$ evaluated during each *j-th* episode. The degradation coefficient is iteratively updated based on the degradation results of the last *j-th* episode. Finally, the degradation coefficient is multiplied by the BESS penalty cost due to ageing $\mathbb{C}_{pen}^{bess}$. It is assumed an annual value of $\mathbb{C}_{pen}^{bess} = \mathbb{C}_{capex}^{bess}/T_{BESS} = 23,533\ [€/MWh]$, calculated as an estimated annualized cost of replacing the battery after the battery's lifespan [59]. The last term is introduced to consider the end-of-life (EOL) criterion. As suggested by Marques et al. [27], an EOL criterion of 70 % of capacity with respect to the initial capacity can be considered a realistic choice for modeling battery degradation in a stationary application. Accordingly, the BESS lifetime considered in this work depends on the number of cycles performed by the battery evaluated by the MILP-based optimization process: the BESS lifetime corresponds to the number of years to reach the EOL criterion of 70 %.

$$\mathbb{C}_{deg}^{bess} = \sum_{t=1}^{T_{BESS}} \mu_{deg,j} \cdot \left[P_{ch-wind}^{bess}(t) + P_{ch-grid}^{bess}(t) + P_{dh}^{bess}(t) \right] \cdot \Delta t \forall t \in T \; [€] \tag{6}$$

Eq. (10), ensures that the sum of the wind farm power losses, the wind farm power generated directly sent to the grid, and the wind farm power generated to charge the battery must be equal to the AC wind farm power generated $P_{gen}^{wind}(t)$ (input historical data) for each time step Δt.

$$\mu_{deg,j} = \left\{ \left[\left(\left(E_{start,j}^{rem} - E_{end,j}^{rem} \right) / 100 \right) \cdot E_{nom}^{bess} \right] \Big/ \sum_{t=1}^{T_j} P_{tot}^{bess}(t) \cdot \Delta t \right\} \cdot \mathbb{C}_{pen}^{bess} \cdot \left(\frac{E_{end,j}^{rem} - EOL}{100 - EOL} \right) \; [€/MWh] \tag{7}$$

$$P_{tot}^{bess}(t) = P_{ch-wind}^{bess}(t) + P_{ch-grid}^{bess}(t) + P_{dh}^{bess}(t) \forall t \in T \; [MW] \tag{8}$$

The Li-ion battery degradation model implemented in this work has been taken and adapted from [24,56]. The remaining capacity expresses the rate of the battery capacity fade based on the battery charging/discharging frequency. The empirical degradation function is defined by the following Eq. (9) and illustrated in Fig. 4. It assumes a 9th-order polynomial behavior, and the EOL criterion considered in this work (70 % with respect to the initial nominal capacity) is reached after 6147 cycles.

$$\begin{aligned} E_{rem}^{bess}(cyc) = {} & 100 - 5.613^{-32} \cdot cyc^9 + 3.121^{-27} \cdot cyc^8 - 6.353^{-23} \cdot cyc^7 \\ & + 6.630^{-19} \cdot cyc^6 - 3.987^{-15} \cdot cyc^5 + 1.435^{-11} \cdot cyc^4 \\ & - 3.070^{-8} \cdot cyc^3 + 3.746^{-5} \cdot cyc^2 - 0.0277 \cdot cyc \; [\%] \end{aligned} \tag{9}$$

To sum up, the degradation penalty function due to battery ageing can be interpreted as a fictitious cost useful to limit the number of cycles performed by the battery. It is introduced in the objective function of the optimization problem to account for the immediate reward for every charging or discharging battery control action during a short period of time considered equal to the time scheduling period $T = 48$ [h].

3.2. Continuous and integer constraints

According to the scheme layout depicted in Fig. 1, the following system power balance equality constraint ensures a balanced operation of the utility-scale wind-battery system. This constraint, expressed by

$$P_{loss}^{wind}(t) + P_{grid}^{wind}(t) + P_{ch-wind}^{bess}(t) = P_{gen}^{wind}(t) \forall t \in T \; [MW] \tag{10}$$

Moreover, the constraint defined by Eq. (11) ensures that the sum between the amount of power generated by the wind farm and sent to the grid and the power discharged by the battery to the grid must be lower or equal to the TSO dispatching orders $P_{ord}^{TSO}(t)$ (input historical data) for each time step Δt.

$$P_{grid}^{wind}(t) + P_{dh}^{bess}(t) \leq P_{ord}^{TSO}(t) \forall t \in T \; [MW] \tag{11}$$

The continuous constraints refer to all those constraints necessary to properly define the dispatching operations of the continuous variables of the MILP-based optimization problem. The constraints defined by Eq. (12–14) ensure that the battery charge from wind, the charge from the grid, and the discharge power flows must be higher or equal to the minimum battery power (set equal to zero) and lower or equal to the maximum battery power, namely the battery nominal power P_{nom}^{bess}, for each time step Δt. The integer variable related to the battery charge from the wind farm $\beta_{ch-wind}^{bess}(t)$, from the grid $\beta_{ch-grid}^{bess}(t)$ and the integer variable associated to the battery discharge $\beta_{dh}^{bess}(t)$, are introduced to prevent charging and discharging processes from occurring simultaneously.

$$0 \leq P_{ch-wind}^{bess}(t) \cdot \beta_{ch-wind}^{bess}(t) \leq P_{nom}^{bess} \forall t \in T \; [MW] \tag{12}$$

$$0 \leq P_{ch-grid}^{bess}(t) \cdot \beta_{ch-grid}^{bess}(t) \leq P_{nom}^{bess} \forall t \in T \; [MW] \tag{13}$$

$$0 \leq P_{dh}^{bess}(t) \cdot \beta_{dh}^{bess}(t) \leq P_{nom}^{bess} \forall t \in T \; [MW] \tag{14}$$

Considering now the energy content of the BESS, the constraint

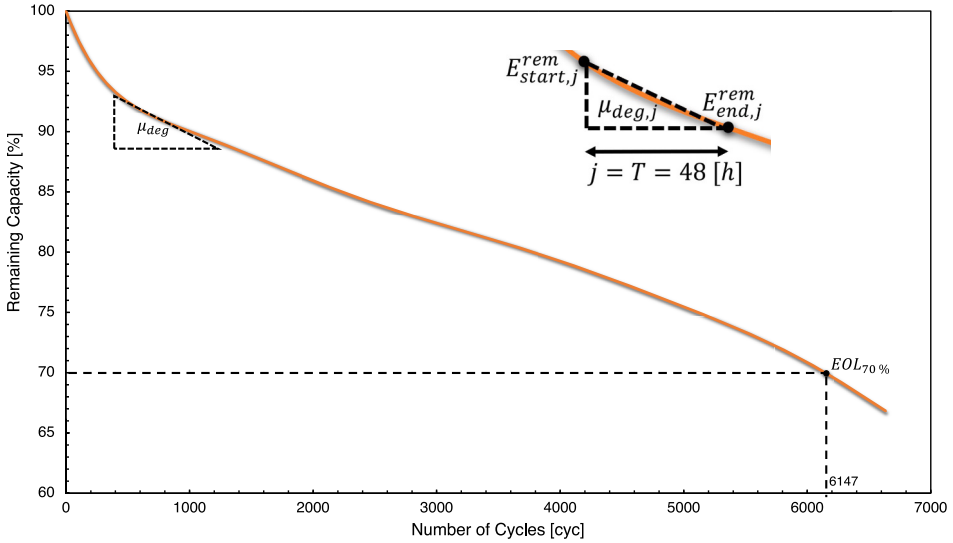

Fig. 4. Empirical degradation function incorporated in the MILP-based optimization problem. The zoom illustrates the degradation coefficient used to evaluate the degradation penalty function due to battery ageing.

expressed by Eq. (15) defines the admissible operative window of the battery state of charge variable $SOC(t)$. Here, it is also considered the remaining capacity at each of the *j-th* episodes. A technical minimum of 20 % of the battery nominal capacity E_{nom}^{bess} is imposed to avoid over-discharge operations that may cause internal failures [60]. The constraint defined in Eq. (16) is split into parts *a* and *b* to account for the first-time step, wherein the state of charge variable assumes a pre-defined value and for every step >1, respectively. This constraint ensures that the battery charge and discharge energy flows translate into the battery state of charge considering the energy stored in the previous time step and the battery operating power. Here, the battery charge from the wind $\eta_{ch-wind}^{bess}$ and from the grid $\eta_{ch-grid}^{bess}$ efficiency, and the battery discharge efficiency η_{dh}^{bess} are introduced to take into account the energy conversion losses occurring during the charge and discharge processes, respectively. Additionally, the self-discharge losses η_{self}^{bess} are considered to take into account the energy conversion losses during idle operations. The MILP-based mathematical model considers the end of optimization time horizon state-of-charge as an initial condition for the next time horizon.

$$0.2\cdot E_{nom}^{bess}\cdot\left(E_{end,j}^{rem}/100\right)\le SOC(t)\le E_{nom}^{bess}\cdot\left(E_{end,j}^{rem}/100\right)\forall t\in T\ [MWh] \tag{15}$$

$$SOC(t)=0.5\cdot E_{nom}^{bess}+\left[P_{ch-wind}^{bess}(t)\cdot\eta_{ch-wind}^{bess}\cdot\Delta t\right]+\left[P_{ch-grid}^{bess}(t)\cdot\eta_{ch-grid}^{bess}\cdot\Delta t\right]-\left[\left(P_{dh}^{bess}(t)/\eta_{dh}^{bess}\right)\cdot\Delta t\right]\forall t\in T:t=0\ [MWh] \tag{16a}$$

$$SOC(t)=SOC(t-1)\cdot\eta_{self}^{bess}+\left[P_{ch-wind}^{bess}(t)\cdot\eta_{ch-wind}^{bess}\cdot\Delta t\right]+\left[P_{ch-grid}^{bess}(t)\cdot\eta_{ch-grid}^{bess}\cdot\Delta t\right]-\left[\left(P_{dh}^{bess}(t)/\eta_{dh}^{bess}\right)\cdot\Delta t\right]\forall t\in T:t\ge 1\ [MWh] \tag{16b}$$

Eq. (17) defines the battery cycle rate variable $cyc_{rate}^{bess}(t)$, namely the fractional cycle rate with respect to a full cycle during the 1-h Δt period [61]. One unit of a full cycle denotes one full charge (from the minimum to the maximum $SOC(t)$ value) and one full discharge (from the maximum to the minimum $SOC(t)$ value).

$$cyc_{rate}^{bess}(t)=\left[\left(P_{ch-wind}^{bess}(t)+P_{ch-grid}^{bess}(t)+P_{dh}^{bess}(t)\right)\cdot\Delta t/E_{nom}^{bess}\right]/2\forall t\in T\ [-] \tag{17}$$

The integers constraints are introduced in the MILP-based optimization problem to ensure that the battery charging and discharging processes do not occur simultaneously at each time step *t*. The integer variable related to the battery charge from the wind process $\beta_{ch-wind}^{bess}(t)$ assumes the value 1 if the BESS charges from the wind farm and 0 otherwise. The same concept is adopted for the battery charging process from the grid, using the binary variable $\beta_{ch-grid}^{bess}(t)$, and for the battery discharging process to the grid, using the binary variable $\beta_{dh}^{bess}(t)$. To correctly bound the integer constraints, it is adopted the *bigM* method [62]. In this work, the artificial variable implemented in the *bigM* method is set to 5,000,000 (i.e., two orders of magnitude greater than any feasible value). Specifically, Eq. (18) describes the first greater-than inequality constraint related to the BESS charging process from the wind farm: if the battery is charging from the grid/discharging to the grid ($\beta_{ch-wind}^{bess}(t)=0$), the battery charging flow from the wind farm $P_{ch-wind}^{bess}(t)$ must be greater than or equal to zero. On the contrary, if the battery is charging from the wind farm ($\beta_{ch-wind}^{bess}(t)=1$), the battery charging flow from the wind farm $P_{ch-wind}^{bess}(t)$ must be greater than or equal to a redundant negative lower limit ($-bigM=-5,000,000$) that is at least two orders of magnitude lower than any feasible value. The same concept for the battery charging from the grid and discharging to the grid processes is adopted in the following Eq. (19–22).

$$P_{ch-wind}^{bess}(t)\ge 0-bigM\cdot\beta_{ch-wind}^{bess}(t)\forall t\in T \tag{18}$$

$$P_{ch-grid}^{bess}(t)\ge 0-bigM\cdot\beta_{ch-grid}^{bess}(t)\forall t\in T \tag{19}$$

$$\left(P_{ch-wind}^{bess}(t)\cdot\beta_{ch-wind}^{bess}\right)+\left(P_{ch-grid}^{bess}(t)\cdot\beta_{ch-grid}^{bess}(t)\right)\le 0+bigM\cdot\left(1-\beta_{dh}^{bess}(t)\right)\forall t\in T \tag{20}$$

$$P_{dh}^{bess}(t)\le 0+bigM\cdot\beta_{dh}^{bess}(t)\forall t\in T \tag{21}$$

$$P_{dh}^{bess}(t)\ge 0-bigM\cdot\left(1-\beta_{ch-wind}^{bess}(t)-\beta_{ch-grid}^{bess}(t)\right)\forall t\in T \tag{22}$$

Finally, the last integer constraint expressed by Eq. (23) ensures that for each time step *t*, the sum between the three integer variables must be lower than or equal to 1. This ensures that the BESS charging and discharging processes cannot simultaneously occur at the same time step *t*.

$$\beta_{ch-wind}^{bess}(t)+\beta_{ch-grid}^{bess}(t)+\beta_{dh}^{bess}(t)\le 1\forall t\in T \tag{23}$$

3.3. Post-processing indicators

In this section, the design, energy, and economic indicators used in this work are defined. These indicators are adopted to provide general criteria for designing the wind-battery system and to assess its techno-economic performance accurately. To provide the generalization of results useful for broader applicability across different scenarios, the indicators are dimensionless, hence they are normalized with respect to their nominal values.

3.3.1. Design indicators

BESS power-to-energy ratio. The BESS power-to-energy ratio r_{p-e}^{bess} is defined as the ratio between the BESS nominal power and the BESS nominal capacity.

$$r_{p-e}^{bess}=\frac{P_{nom}^{bess}}{E_{nom}^{bess}}\left[\frac{MW}{MWh}\right] \tag{24}$$

BESS cumulative number of cycles. The BESS cumulative number of cycles is evaluated by summing hour by hour the battery cycle rate variable $cyc_{rate}^{bess}(t)$, previously defined by Eq. (17).

3.3.2. Energy indicators

Wind farm annual capacity factor. The wind farm's annual capacity factor cf_{wind} is defined in percentage terms as the ratio between the sum of the wind farm power production hour-by-hour and the theoretical maximum wind farm power production over the selected year.

$$cf_{wind}=\frac{\sum_{t=1}^{8760}P_{gen}^{wind}(t)\cdot\Delta t}{P_{nom}^{wind}\cdot 8760}\cdot 100\left[\frac{\%}{year}\right] \tag{25}$$

BESS annual capacity factor. The BESS annual capacity factor cf_{bess} is defined in percentage terms as the ratio between the sum of the battery state of charge hour-by-hour and the theoretical maximum wind farm power production over the selected year, considering the BESS operational range window of 80 %.

$$cf_{bess}=\frac{\sum_{t=1}^{8760}SOC(t)\cdot\Delta t}{E_{nom}^{bess}\cdot 0.80\cdot 8760}\cdot 100\left[\frac{\%}{year}\right] \tag{26}$$

Wind farm annual curtailed energy. The wind farm annual curtailed energy s_{curt}^{wind} represents the fraction in percentage terms of the annual wind farm curtailed energy with respect to the total AC power generated by the wind farm over the selected year

$$s_{curt}^{wind} = \frac{\sum_{t=1}^{8760} P_{loss}^{wind}(t)\cdot\Delta t}{\sum_{t=1}^{8760} P_{gen}^{wind}(t)\cdot\Delta t}\cdot 100\ \left[\frac{\%}{year}\right] \tag{27}$$

Wind-to-BESS share. The wind-to-BESS share s_{bess}^{wind} represents the fraction in percentage terms of the power generated from the wind and sent to charge the battery with respect to the total AC power generated by the wind farm over the selected year.

$$s_{bess}^{wind} = \frac{\sum_{t=1}^{8760} P_{ch-wind}^{bess}(t)\cdot\Delta t}{\sum_{t=1}^{8760} P_{gen}^{wind}(t)\cdot\Delta t}\cdot 100\ \left[\frac{\%}{year}\right] \tag{28}$$

Wind-to-grid share. The wind-to-grid share s_{grid}^{wind} represents the fraction in percentage terms of the power generated from the wind and sent to the grid with respect to the total AC power generated by the wind farm over the selected year.

$$s_{grid}^{wind} = \frac{\sum_{t=1}^{8760} P_{grid}^{wind}(t)\cdot\Delta t}{\sum_{t=1}^{8760} P_{gen}^{wind}(t)\cdot\Delta t}\cdot 100\ \left[\frac{\%}{year}\right] \tag{29}$$

3.3.3. Economic indicators

Net Present Value. The net present value economic parameters (*NPV* in €) is calculated as the difference between the discounted cumulative revenue $\mathbb{R}_{cum}^{bess}$ from the BESS and the BESS lifetime cumulative cost $\mathbb{C}_{cum}^{bess}$ of the BESS over the project lifetime, assumed equal to the BESS lifetime ($T_{BESS} = 15\ [years]$). The cumulative BESS revenue stream $\mathbb{R}_{exp}^{bess}$ was previously defined in Eq. (3), discounted up to the BESS lifetime. While the BESS lifetime cumulative cost is composed of the investment cost $\mathbb{C}_{capex}^{bess}$, the operation and management cost $\mathbb{C}_{opex}^{bess}$, and the import cost due to importing energy from the grid to the battery $\mathbb{C}_{imp}^{bess}$. The investment cost is assumed to occur in the first year (zeroth year), while the other two components are discounted up to the BESS lifetime. Notably, only the BESS cash flows are considered in the NPV definition, as the objective of the conducted techno-economic analysis is to determine the profitability of integrating a BESS into an existing wind farm based on the specific case study and assumptions used in this work.

$$NPV = \sum_{n=1}^{T_{BESS}} \frac{\mathbb{R}_{exp}^{bess}}{(1+r)^n} - \left(\mathbb{C}_{capex}^{bess} + \sum_{n=1}^{T_{BESS}} \frac{\mathbb{C}_{opex}^{bess}}{(1+r)^n} + \sum_{n=1}^{T_{BESS}} \frac{\mathbb{C}_{imp}^{bess}}{(1+r)^n}\right) = \mathbb{R}_{cum}^{bess} - \mathbb{C}_{cum}^{bess}\ [€] \tag{30}$$

Levelized cost of storage. The levelized cost of storage (*LCOS* in €/*MWh*) for wholesale energy arbitrage application, defined by Schmidt et al. [63], defines the discounted cost per unit of discharged electricity for a specific storage technology (in this work Li-ion battery energy storage system), and for a specific application (in this work wholesale energy arbitrage service). The following *LCOS* equation incorporates all elements required to evaluate the whole lifetime cumulative cost of the BESS technology $\mathbb{C}_{cum}^{bess}$: investment cost $\mathbb{C}_{capex}^{bess}$, operation and management cost $\mathbb{C}_{opex}^{bess}$, import cost due to importing energy from the grid to the battery $\mathbb{C}_{imp}^{bess}$, divided by the total BESS energy discharged during the investment period. The total BESS energy discharged component $E_{dh.tot}^{bess}$ is calculated by summing hour-by-hour the BESS discharge power flow $P_{dh}^{bess}(t)$ for each time step Δt over 1-year of dispatch operations up to the BESS lifetime. It is assumed that the investment cost incurred in the first year and the sums ongoing costs in each year (n) up to BESS lifetime (T_{BESS}), discounted by the discount rate (r) [63].

$$\text{LCOS} = \frac{\mathbb{C}_{\text{capex}}^{\text{bess}} + \sum_{n=1}^{T_{BESS}} \frac{\mathbb{C}_{\text{opex}}^{\text{bess}}}{(1+r)^n} + \sum_{n=1}^{T_{BESS}} \frac{\mathbb{C}_{\text{imp}}^{\text{bess}}}{(1+r)^n}}{\sum_{n=1}^{T_{BESS}} \frac{E_{\text{dh,tot}}^{\text{bess}}}{(1+r)^n}} = \frac{\mathbb{C}_{\text{cum}}^{\text{bess}}}{\sum_{n=1}^{T_{BESS}} \frac{E_{\text{dh,tot}}^{\text{bess}}}{(1+r)^n}}\ \left[\frac{€}{\text{MWh}}\right] \tag{31}$$

Interest Rate of Return. The interest rate of return (*IRR* in percentage terms) gives a measure of return on investment, and it can be calculated by setting *NPV* to zero. *IRR* is effectively the new discount rate that gives *NPV* of zero over the whole BESS lifetime.

$$\text{NPV} = \sum_{n=1}^{T_{BESS}} \frac{\mathbb{R}_{\text{exp}}^{\text{bess}}}{(1+\text{IRR})^n} - \mathbb{C}_{\text{cum}}^{\text{bess}} = 0\ [€] \tag{32}$$

Payback time. The payback time period (*PBT* in years) is defined as the period of time when the difference between the BESS cumulative revenue and the BESS cumulative cost is equal to zero.

$$\sum_{n=0}^{PBT} \mathbb{R}_{cum}^{bess} = \sum_{n=0}^{PBT} \mathbb{C}_{cum}^{bess} \tag{33}$$

These economic indicators are evaluated over the entire lifetime of the project ($T_{BESS} = 15\ [y]$ [64]). The first year (zeroth year) is considered the installation and commissioning year, followed by 15 years of operation. All the costs and revenues are discounted across all 15 years of operation, considering a discount rate equal to $r = 5\%$ [65]. Table 3 shows the BESS cost breakdown considered in this work. The costs are broken down into CAPEX (capital expenditure) and OPEX (operating expenditure). These costs were taken and adapted from [66].

4. Results and discussion

This section presents and discusses the most relevant design, energy, and economic results obtained by the optimal participation of the wind farm and BESS in the Italian wholesale day-ahead electricity market. Firstly, Section 4.1 presents the optimal BESS size obtained by the long-term profitability analysis. Secondly, in Section 4.2 the optimal scheduling operations of the wind-battery system considering the BESS optimal size were presented. Finally, Section 4.3, is centered on the sensitivity analysis for the optimized BESS size.

4.1. Optimal BESS size

This section presents the optimal BESS size obtained through the MILP-based optimization process implemented in this work. The economic indicator used to determine the optimal size is the NPV, defined

Table 3
BESS cost breakdown.[a] Source: [66].

CAPEX	[€/kWh]	% of CAPEX	OPEX	[€/kWh]	% of CAPEX
Li-ion battery	173.7	49 %	Operating and maintenance cost (per year)	10.6	3 %
Battery central inverter	13.9	4 %			
Structural BOS	22.2	6 %			
Electrical BOS	48.1	14 %			
Installation labor & equipment	25.9	7 %			
EPC overhead + sales tax	27.7	8 %			
Developer cost + profit	40.7	12 %			
Total CAPEX	**353**				

[a] Average annual energy exchange for year 2023 (0.9241 €/$) was used to convert costs from $ to € [68].

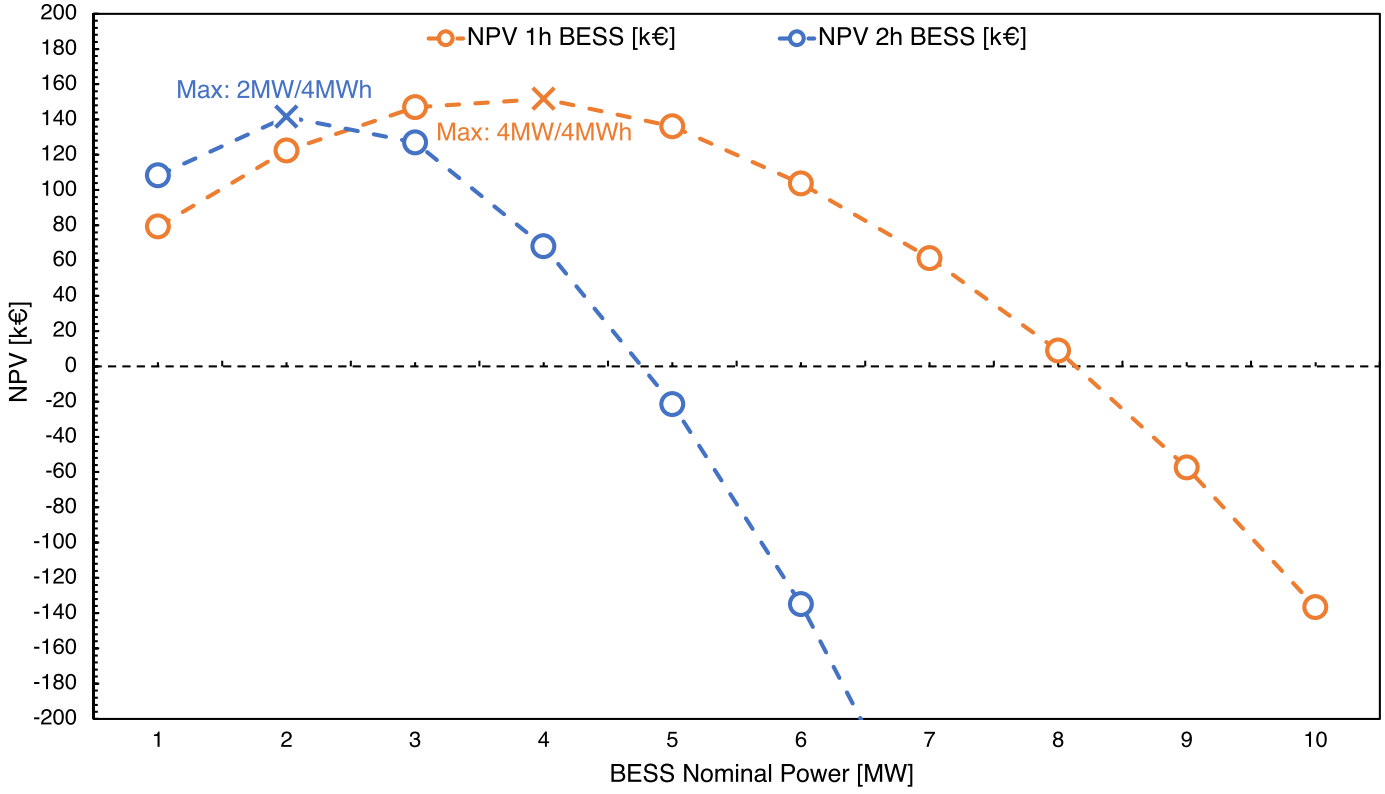

Fig. 5. NPV of the BESS investment as a function of different BESS sizes.

Table 4
Tabular representation of results illustrated in Fig. 5.

BESS Nominal Power [MW]	1	2	3	4	5	6	7	8	9	10
NPV 1 h BESS [K€]	79.25	122.26	146.92	151.72	136.07	103.62	61.36	8.90	−57.47	−136.74
NPV 2 h BESS [K€]	108.23	141.54	126.97	68.01	−21.53	−134.96	−275.29	−441.60	−630.86	−825.70

by Eq. (30). As illustrated in Fig. 5, the highest NPV of 152 k€ is achieved with a 1-h BESS of 4 MW / 4 MWh. For a 2-h configuration, the highest NPV of 142 k€ is reached with a BESS size of 2 MW / 4 MWh. The trend indicates that the 2-h configuration (blue curve) reaches negative NPV values sooner than the 1-h configuration (orange curve). Specifically, a negative NPV of −22 k€ is reached with a BESS size of 5 MW /10 MWh, while a negative NPV of −58 k€ is reached with a BESS size of 9 MW /9 MWh. A tabular representation of the NPV values at different BESS sizes is reported in Table 4. These results suggest that in this case study, a 1-h BESS of 4 MW / 4 MWh integrated with the wind farm under investigation will yield the highest profitability over the BESS lifetime of 15 years in terms of NPV. Therefore, in the subsequent sections, the optimal BESS size is considered to be 4 MW/4 MWh. This BESS performs on average of approximately 380 cycles per year, equating to about 1.04 cycles per day. Further details on wind-BESS scheduling operations are provided in the next Section 4.2.

The optimal BESS sizes determined in this study are consistent with those reported in [42], where a multi-objective model was developed for the optimal configuration of a BESS integrated with a PV-wind system. In that study, a wind farm with a rated capacity of 20 MW, a PV plant with a rated capacity of 20 MW, and a BESS with a rated capacity of 2 MW were considered. The maximum annual net revenue of the BESS, while providing both energy arbitrage and reserve ancillary services, was found to be 2 MW /4 MWh. Moreover, the study highlighted that the monthly revenue of the BESS is significantly higher in the wholesale energy arbitrage market compared to the reserve ancillary services market. Specifically, the monthly revenue from energy arbitrage ranged from 10,216 €[a] to 13,570 €[a], while the monthly revenue from reserve ancillary services ranged from 1915 €[a] to 2227 €[a]. Another consistent result with our study is reported in [44]. In this work it is examined the participation of a wind farm coupled with a hybrid battery energy storage system (HESS) in the day-ahead and the automatic frequency restoration reserve markets. The HESS is composed of a lithium-ion and a redox flow battery. For a 10 MW wind farm, the optimal battery configuration consists of a hybrid system comprising a 1 MW/1 MWh lithium-ion battery and a vanadium redox flow battery with a negligible capacity.

Table 5
Net profit [k€/year] from arbitrage operations of a wind farm without BESS (W/O) and with BESS (4 MW/4MWh).

	W/O BESS	With BESS
Wind revenue stream [k€/year]	10,999	10,880
BESS net profit [k€/year]	/	190.353
Net Profit [k€/year]	**10,999**	**11,071**

Table 5 presents the results in terms of annual net profit for both the standalone wind farm and the wind farm integrated with the BESS. The system without BESS consists solely of the wind farm. Conversely, the system with battery storage includes the wind farm and the optimally sized BESS of 4 MW/4 MWh. The wind revenue stream is evaluated according to Eq. (2) by multiplying the wholesale energy price by the wind-to-grid power flow for each time step, considering the dispatch orders. The BESS net profit is calculated as the difference between the

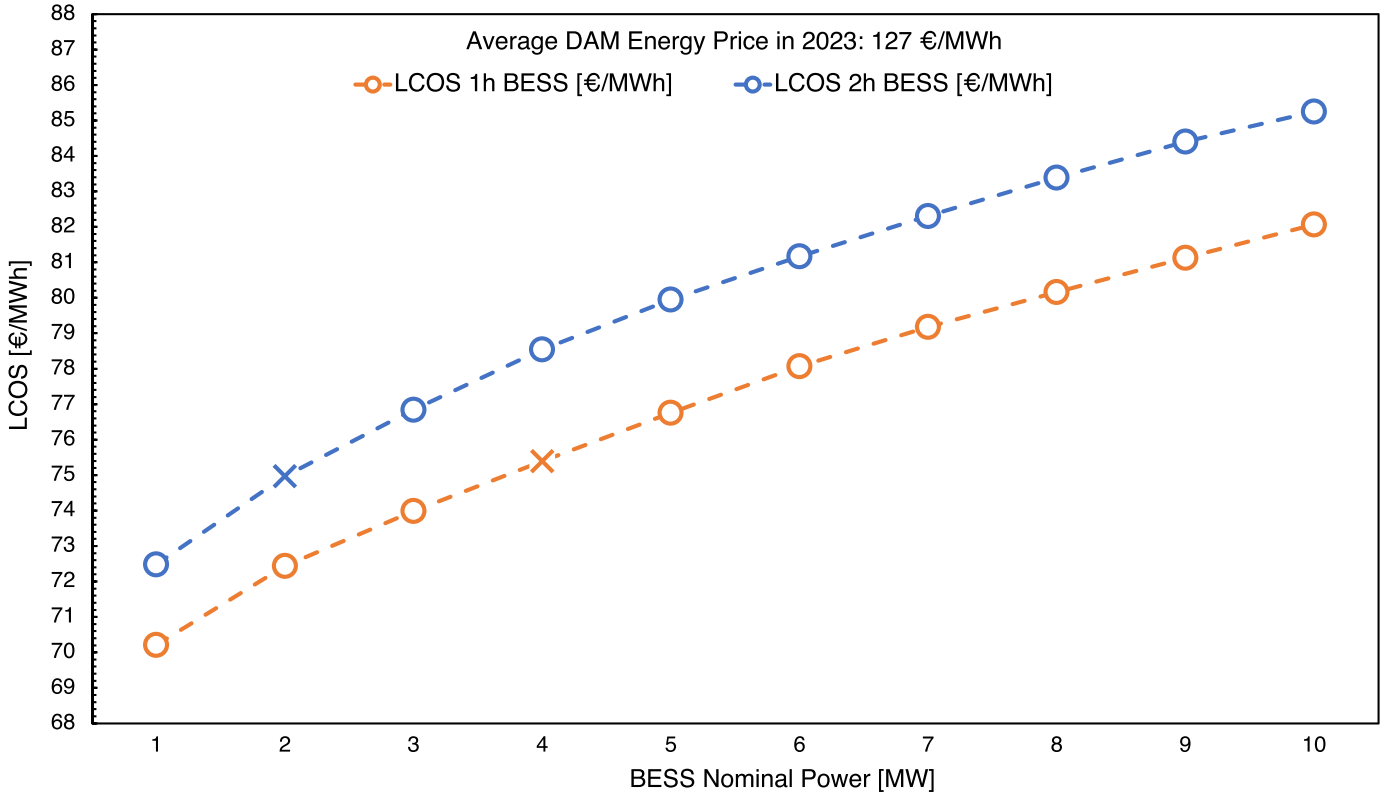

Fig. 6. LCOS of the BESS investment as a function of different BESS sizes.

BESS revenue component (Eq. (3)), which is the wholesale energy price multiplied by the BESS discharge power flow for each time step, and the BESS import cost component (Eq. (4)), defined as the wholesale energy price multiplied by the BESS charge flow from the grid for each time step. These components are evaluated at each time step ($\Delta t = 1\ [h]$) over the BESS lifetime ($T_{BESS} = 15\ [y]$. The annual value in Table 5 refers to the average value over these 15 years of simulated operations. The results demonstrate a modest increase in annual revenue of approximately 190 k€ from the wind farm-BESS system compared to the system consisting solely of the wind farm. A consistent result is obtained in [43], where authors found a benefit of the wind farm with BESS of 15.74 k€ per year compared to the wind farm without BESS. The main difference compared to our study is that they considered only two weeks as observation periods.

Fig. 6 presents the LCOS economic indicator, defined in Eq. (31), as a function of different BESS sizes analyzed. The orange curve represents the 1-h BESS configuration, while the blue curve corresponds to the 2-h BESS configuration. The LCOS trend increases with larger BESS sizes, indicating that the increase in the cumulative lifetime cost of the BESS technology (the numerator of the LCOS formula) has a greater impact than the increase in the total BESS energy discharged during the investment period (denominator of the LCOS formula). Considering the optimal BESS sizes of 4 MW / 4 MWh and of 2 MW / 4 MWh, it is obtained an LCOS value of 75.4 €/MWh and 75.0 €/MWh, respectively. Globally, all LCOS values obtained by the MILP-based simulations are lower than the average DAM energy price in 2023, which is 127 €/MWh. A tabular representation of the LCOS values at different BESS sizes is reported in Table 6. This trend suggests that integrating a BESS into the existing wind farm under investigation could be a sound investment based on the assumptions of this case study. However, this comparison is between LCOS values and the average DAM energy price of 2023, which does not account for the volatility of DAM energy prices. Given that energy price volatility is a major factor in making the energy arbitrage service profitable [56], the LCOS metric may not be the most suitable measure for determining the optimal size for maximum profitability from the energy arbitrage service.

The following Fig. 7 shows the IRR economic metric defined in Eq. (32) as a function of different BESS sizes analyzed. The presented results, represented by two distinct curves, delineate the declining trend of IRR as the nominal power of the BESS increases from 1 to 10 MW. The orange curve corresponds to the 1-h BESS configuration, while the blue curve corresponds to the 2-h BESS configuration. Both curves exhibit a downward trajectory, indicating a decrease in economic return with increasing BESS capacity. Specifically, the IRR starts at approximately 7.5–8.5 % for a 1 MW BESS in both configurations and decreases to around 3.5–4.5 % for the 10 MW BESS, with the 1-h configuration consistently offering a higher IRR than the 2-h configuration. A tabular representation of the IRR values at different BESS sizes is reported in Table 7. This suggests that smaller BESS capacities are more economically viable in terms of return on investment for the scenarios considered in this study. The optimal BESS sizes of 4 MW / 4 MWh and 2 MW / 4 MWh present an IRR value of 6.6 % and 6.5 %, respectively. As pointed out by Judge et al. [65], IRR values may be required to meet a hurdle rate of 8–9 % for renewable energy projects to be financially viable. The

Table 6
Tabular representation of results illustrated in Fig. 6.

BESS Nominal Power [MW]	1	2	3	4	5	6	7	8	9	10
LCOS 1 h BESS [€/MWh]	70.21	72.44	73.99	75.39	76.76	78.07	79.18	80.16	81.13	82.07
LCOS 2 h BESS [€/MWh]	72.48	74.97	76.85	78.55	79.95	81.17	82.31	83.39	84.40	85.25

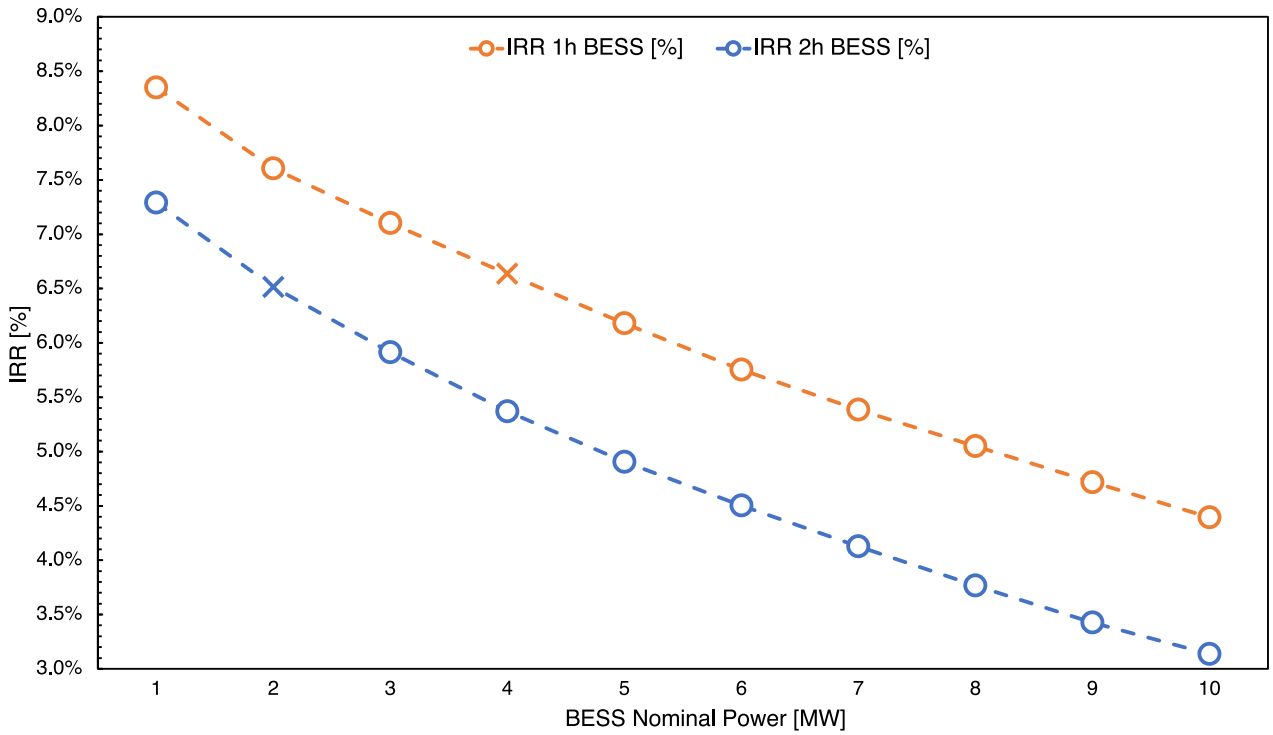

Fig. 7. IRR of the BESS investment as a function of different BESS sizes.

Table 7
Tabular representation of results illustrated in Fig. 7.

BESS Nominal Power [MW]	1	2	3	4	5	6	7	8	9	10
IRR 1 h BESS [%]	8.35	7.61	7.10	6.64	6.18	5.75	5.38	5.05	4.72	4.39
IRR 2 h BESS [%]	7.29	6.51	5.91	5.37	4.91	4.50	4.13	3.77	3.43	3.14

obtained IRR values present a value close to the hurdle rate, especially for lower BESS power-to-energy ratios, indicating that the integration of the BESS into the existing wind farm under investigation is financially viable.

In conclusion, the last two plots visualize the year-by-year cumulative NPV for different BESS sizes over the assumed BESS lifetime of $T_{BESS} = 15$ [*years*]. Fig. 8 (a) shows the cumulative NPV considering the 1-h BESS configuration, while Fig. 8 (b) shows the cumulative NPV considering the 2-h BESS configuration. Each line represents a specific power and energy capacity combination, indicated by diverse colors. There is evidence of a common trend between the two plots: the lower power-to-energy configurations, such as the 1 MW / 1 MWh and 1 MW / 2MWh configurations, start with a negative NPV value and remain fairly consistent. On the contrary, comparing the lower with the larger power-to-energy configurations, such as 10 MW / 10 MWh and 10 MW / 20 MWh, they begin at much lower negative NPV values, indicating higher initial costs or lower short-term returns but displaying lesser negative slope over time. These slopes suggest that the rate of increase in NPV over time is more favorable compared to those with equivalent power but lower energy capacities. From a long-term perspective, besides the assumed BESS lifetime of 15 years, this behavior suggests that a BESS with higher energy capacities might offer better long-term economic benefits, despite larger initial investments.

Furthermore, these plots illustrate the payback time (PBT) metric of the different BESS configurations previously defined in Eq. (33). Notably, the 1 MW / 1 MWh and 1 MW / 2 MWh configurations exhibit the shortest payback times, at approximately 10.8 and 11.9 years, respectively. Additionally, the last configurations to achieve payback within the 15-year lifespan of the BESS are the 8 MW / 8 MWh and 4 MW / 8 MWh setups, with payback times of 14.9 and 14.4 years, respectively. A tabular representation of the PBT values at different BESS sizes is reported in Table 8. This analysis reveals that configurations with a 1-h discharge duration generally present more options yielding positive NPV values post-BESS lifetime compared to the 2-h configurations.

In summary, the results reported in these plots elucidate the economic impact of different BESS sizes over their operational life, emphasizing the trade-off between initial investment costs and long-term profitability.

Table 9 summarizes all the design, energy, and economic indicators defined previously from Eq. (24) to Eq. (33) for the different BESS sizes analyzed. These values correspond to an average over these 15 years of simulated operations.

4.2. Wind-BESS optimal scheduling operations

This section presents the optimal scheduling operations of the wind-BESS system under investigation as simulated by the proposed MILP-based model. Fig. 9 illustrates the system scheduling in response to an energy dispatching order, which indicates periods of wind curtailment. The wind-to-grid power flow (green bars) represents the wind power delivered to the grid, the wind-to-BESS power flow (blue bar) denotes the wind power used to charge the battery, and the BESS-to-grid power flow (red bar) reflects the power discharged from the battery to the grid. The battery's state of charge (SOC, grey curve), wind power production (light blue curve), and grid power admission (violet curve) are expressed in percentage terms and refer to the right axis.

It is worth noting that the grid power admission provided by the Italian Transmission System Operator (TSO) varies from 0 to 100 %. A

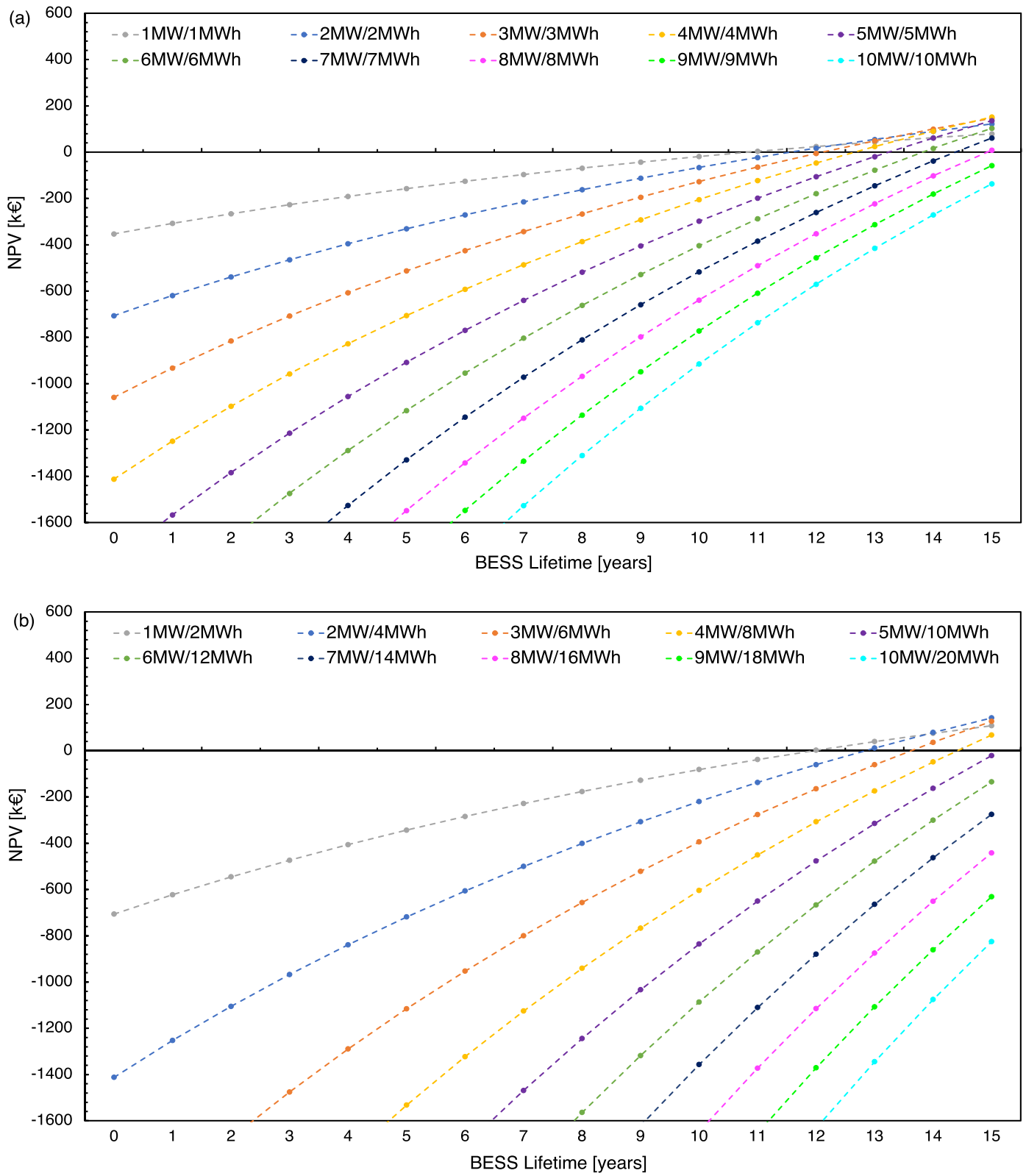

Fig. 8. Cumulative NPV of the BESS investment as a function of different BESS sizes considering a 1-h configuration (a), and a 2-h configuration (b).

value of 0 % indicates complete curtailment of wind power for that hour due to grid congestion, necessitating the shutdown of wind farm turbines. Values between 0 and 100 % indicate partial load operation, where although the wind turbines can generate at nominal power, their output must be limited. This partial operation might be necessitated by maintenance activities on individual turbines. Conversely, a grid power admission of 100 % indicates the absence of any dispatch orders from the TSO, allowing power delivery up to the combined nominal capacities of the wind farm and BESS. The integration of a BESS is advantageous during periods with dispatching orders, as it allows for wind-generated

Table 8
Tabular representation of results illustrated in Fig. 8.

BESS Nominal Power [MW]	1	2	3	4	5	6	7	8	9	10
PBT 1 h BESS [year]	10.83	11.56	12.10	12.65	13.24	13.82	14.38	14.92	>15	>15
PBT 2 h BESS [year]	11.95	12.84	13.62	14.42	>15	>15	>15	>15	>15	>15

Table 9
Design, energy, and economic indicators for optimal BESS sizes of 4 MW/4MWh and 2 MW/4MWh.

Design indicators	BESS power-to-energy ratio [MW/MWh]	4/4	2/4
	Annual BESS number of cycles [cyc]	397	380
Energy indicators	Wind farm annual capacity factor [%/year]	26.2	26.2
	BESS annual capacity factor [%/year]	55.5	56.3
	Wind farm annual curtailed energy [%/year]	2.2	2.2
	Wind-to-BESS share [%/year]	1.4	1.4
	Wind-to-Grid share [%/year]	96.4	96.4
Economic indicators	Net Present Value (NPV) [k€]	151.7	141.5
	Levelized Cost of Storage (LCOS) [€/MWh]	75.4	75.0
	Interest Rate of Return (IRR) [%]	6.6	6.5
	Payback Time Period (PBT) [years]	12.7	12.8

electricity to be stored rather than curtailed.

As depicted in Fig. 9, during hours where both wind resources (light blue curve) and dispatch orders (violet curve) coexist, the generated wind power is utilized to charge the BESS (blue bar), preventing potential energy waste. In this specific setup, considering the optimal BESS size of 4 MW / 4 MWh, the wind-to-BESS power is capped at the nominal BESS capacity of 4 MW. Consequently, the SOC profile (grey curve) escalates from its technical minimum (20 % of its nominal capacity) to its maximum (100 % minus energy losses due to degradation after 2726 h of operation), demonstrating the effective formulation of the MILP model to maximize the utility of the battery and recuperate all wind energy susceptible to curtailment.

Given that wind curtailment is a rare phenomenon (as indicated in Table 2, this case study considers a wind curtailment of approximately 2.2 % of the annual wind farm production), it was deemed reasonable to broaden the utilization of the BESS by incorporating wholesale energy arbitrage. This approach generates additional profits, as the battery is charged not only from curtailed wind energy but also from wind-generated energy during periods of low energy prices. Consequently, the battery undergoes a significantly higher number of cycles, thereby optimizing its utilization. The fundamental principle of energy arbitrage involves generating revenue by charging the battery during low-price periods (valley periods) and discharging it back to the grid during high-price periods (peak periods). This strategy exploits energy price volatility to generate profits from battery dispatch operations. This application is depicted in Fig. 10.

In Fig. 10 (a), the battery charging and discharging power flows are shown in [MW] and refer to the left axis: wind to BESS charging power flow (blue bars), grid to BESS charging power flow (orange bars), and BESS to grid discharging power flow (red bars). The 2023 day-ahead market (DAM) electricity prices (yellow curve) are expressed in [€/MWh] and refer to the right axis. Fig. 10 (b) presents the wind power (light blue curve), grid power admission (violet curve), and battery state of charge (SOC, grey curve) as percentages over the same period depicted in the previous figure.

The plots highlight the core principle of energy arbitrage: during periods of low energy prices (valley periods), the BESS stores energy (SOC increases) from the wind farm if wind resources are available and from the grid if they are not (as shown by the orange bar at time 2498

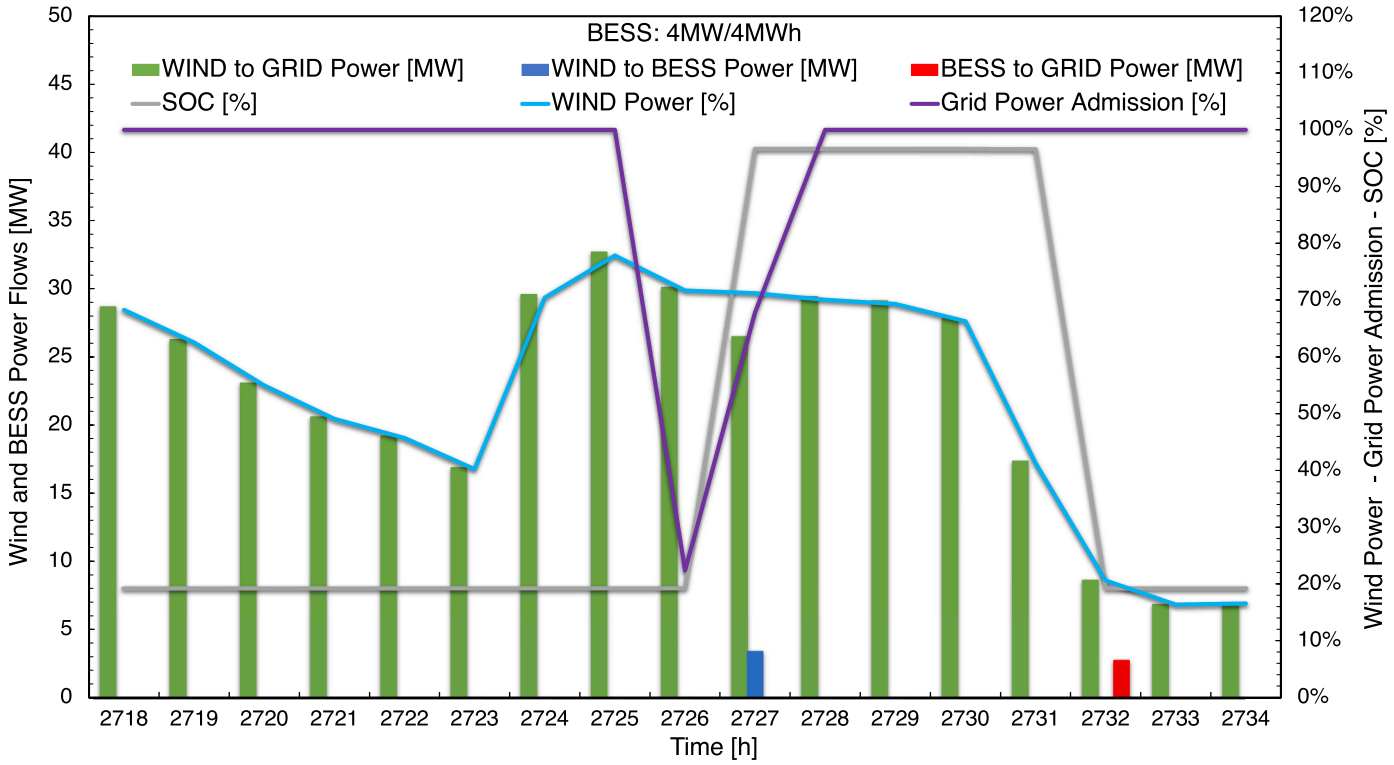

Fig. 9. Wind-BESS optimal scheduling operations during wind curtailment.

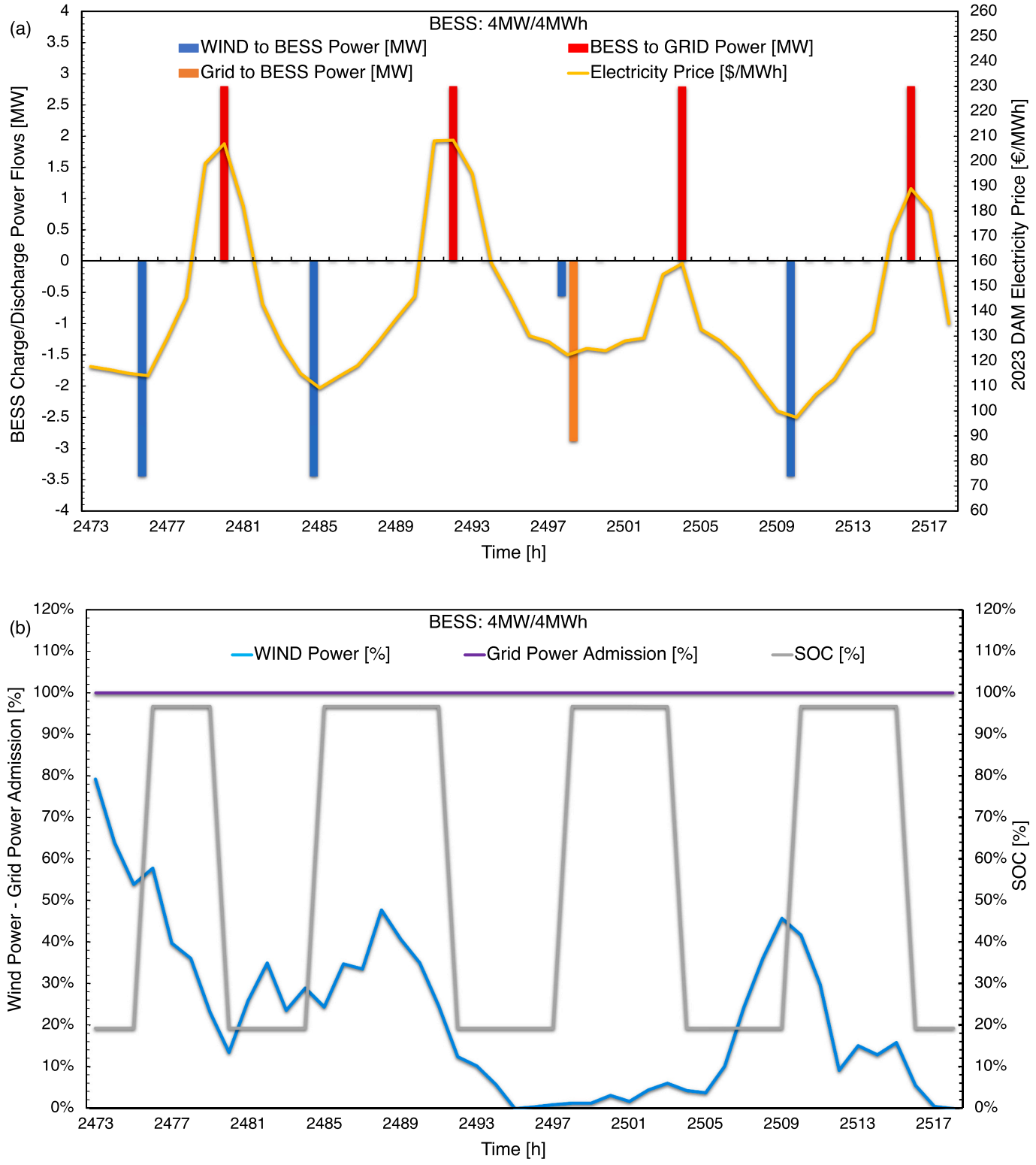

Fig. 10. Wind-BESS optimal scheduling operations considering the wholesale energy arbitrage application.

[h]). Conversely, during periods of high energy prices (peak periods), the BESS discharges energy (SOC decreases). Overall, analyzing these scheduling operations is crucial for validating the MILP-based optimization model implemented in this work.

Fig. 11 depicts the battery state of charge (SOC) profile (blue area, left axis) expressed as a percentage and the number of cycles performed by the battery (orange curve, right axis) over the entire simulation period, which corresponds to the BESS lifetime of 15 years (131,400 h). The chart clearly demonstrates a gradual decrease in battery capacity from 100 % to the end-of-life (EOL) criterion of 70 %, alongside a concurrent progressive increase in the number of cycles, which contributes to capacity fade. This highlights the necessity of incorporating a cycle-counting degradation model to account for capacity degradation accurately.

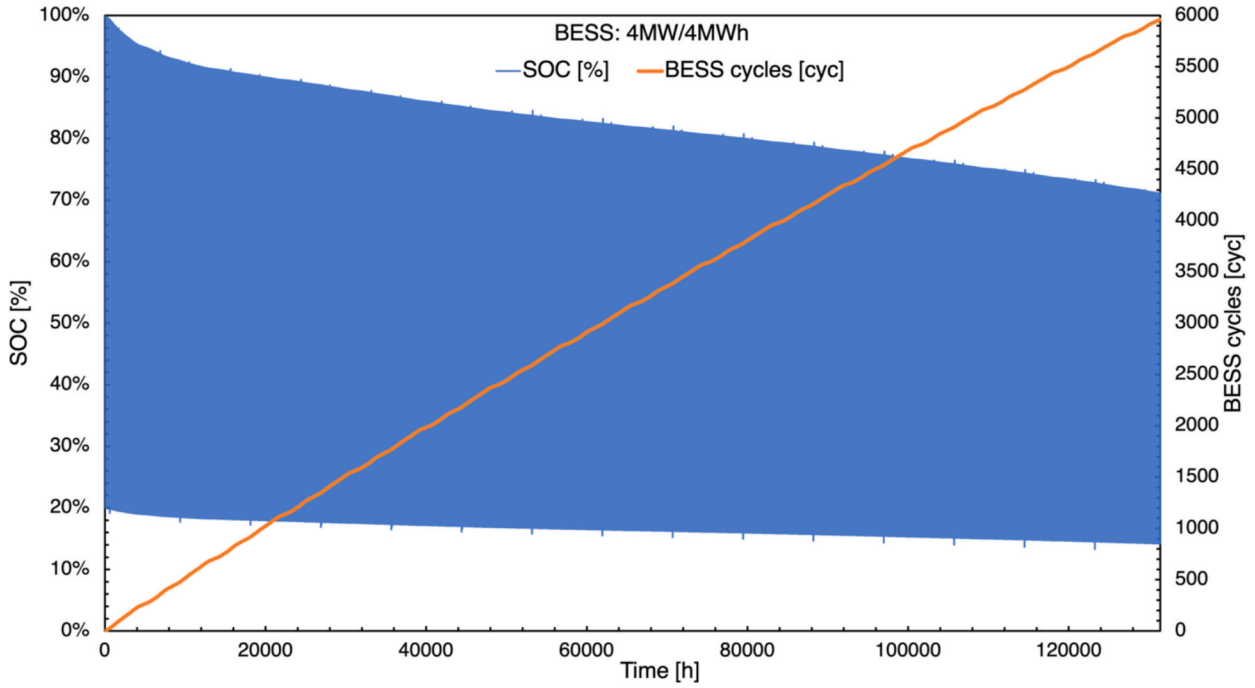

Fig. 11. SOC profile and number of cycles of the BESS along the whole BESS lifetime of 15 years.

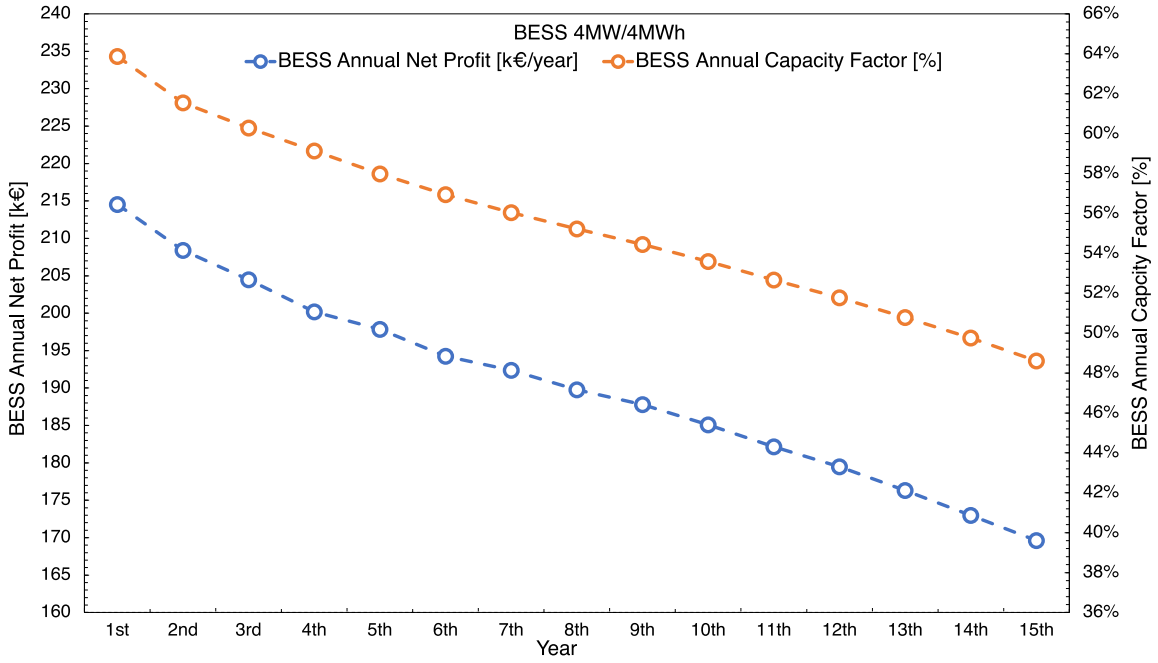

Fig. 12. BESS annual net profit and BESS annual capacity factor along the 15-year battery lifetime.

A key innovation of this work is the consideration of an updated SOC value after each simulation process, as defined in the constraint expressed by Eq. (15). This approach enables the generation of realistic battery power flow values, reflecting the cycle-by-cycle decrease in battery capacity and the consequent reduction in the amount of energy that can be exchanged through the grid. Specifically, considering the optimal BESS size of 4 MW / 4 MWh, after 15 years of operation, the BESS capacity declines from 100 % to 72.5 %. At this point, the battery has completed 5694 cycles, which corresponds to approximately 380 cycles per year, or 1.04 cycles per day.

The effect of battery capacity fade on profitability is illustrated in Fig. 12, which presents the BESS annual net profit (blue curve, left axis) expressed in [k€/year]. The BESS annual capacity factor (orange curve, right axis) is expressed as a percentage and defined by Eq. (26) over the 15-year BESS lifetime. The chart clearly demonstrates a gradual decline in battery performance from a techno-economic perspective. The BESS annual net profit decreases from approximately 215 k€ in the first year to around 170 k€ in the fifteenth year, representing a reduction of about 45 k€. In percentage terms, the BESS profits in the fifteenth year have reduced by approximately 20.9 % compared to the first year. Similarly, the BESS annual capacity factor decreases from approximately 64 % in the first year to about 49 % in the fifteenth year, corresponding to a total

Table 10
Tabular representation of results illustrated in Fig. 12.

Year	BESS annual net profit [k€/year]	BESS annual capacity factor [%]
1st	214.55	63.87
2nd	208.40	61.55
3rd	204.48	60.29
4th	200.18	59.13
5th	197.86	57.99
6th	194.25	56.95
7th	192.37	56.05
8th	189.77	55.22
9th	187.78	54.45
10th	185.08	53.59
11th	182.16	52.67
12th	179.49	51.78
13th	176.30	50.79
14th	172.99	49.75
15th	169.63	48.61

reduction of about 15 %. A tabular representation of the BESS annual net profit and BESS annual capacity factor over the 15-year lifetime is reported in Table 10. These results confirm that the amount of energy exchanged by the battery, and hence its capacity, is linked to net profit. Therefore, to obtain realistic profitability evaluations, it is essential to consider the degradation effect due to battery ageing. The BESS annual net profit decrement along its lifetime presented in Fig. 12 is consistent with the results obtained in [43]. In the economic assessment of day-ahead price arbitrage by the wind fam BESS, the authors found that the BESS benefits in the last years have reduced by 30.5 % compared to the first year.

4.3. Sensitivity analysis

In this section, sensitivity analyses were carried out for the optimized BESS size of 4 MW / 4 MWh on battery capital expenditure costs, battery efficiency, and wind-casted energy to properly understand the impact of slight changes in technical and economic parameters.

4.3.1. Battery capital expenditure cost

Fig. 13 illustrates the impact of BESS capital expenditure (CAPEX) on both the net present value (NPV) and internal rate of return (IRR), considering the optimized BESS size of 4 MW/4 MWh. In this sensitivity analysis, all parameters of the MILP-based power-energy model were kept constant. The NPV, represented by the blue curve, refers to the left axis, and the IRR, represented by the orange curve, refers to the right axis. These economic indicators are plotted against varying BESS costs, ranging from 125 €/kWh to 350 €/kWh in steps of 25 €/kWh. In the case study discussed in Section 4.1 and in Section 4.2, a battery cost of 350 €/kWh was assumed, as indicated in Table 3.

The results demonstrate a clear inverse relationship between BESS CAPEX and both NPV and IRR. As the cost per kWh increases, both NPV and IRR decrease significantly, reflecting the reduced profitability of the investment. At lower BESS costs, the NPV is higher, indicating more favorable returns. For instance, at 125 €/kWh, the NPV is around 1320 k€, and the IRR reaches approximately 35 %, with a payback time (PBT) of around 3 years. Conversely, as the BESS cost increases to 325 €/kWh, the NPV declines to approximately 271 k€, with an IRR of about 8 % and a PBT of around 11.5 years. A tabular representation of the NPV and IRR values at different BESS CAPEX costs is reported in Table 11. As discussed in Section 4.1, IRR values may be required to meet a hurdle rate of 8–9 % for renewable energy projects to be financially viable [65]. This minimum hurdle rate is reached at a BESS CAPEX of 325 €/kWh. Therefore, to be financially viable for the renewable project under investigation (i.e., integrating a battery into the existing wind farm), the battery cost will need to be below 325 €/kWh, as demonstrated in Fig. 13.

An additional insight from this plot is the linear trend observed in NPV as the battery cost varies. Specifically, every 25 €/kWh reduction in BESS CAPEX corresponds to an improvement in NPV of approximately 131 k€. In contrast, the IRR exhibits a non-linear trend, which is more

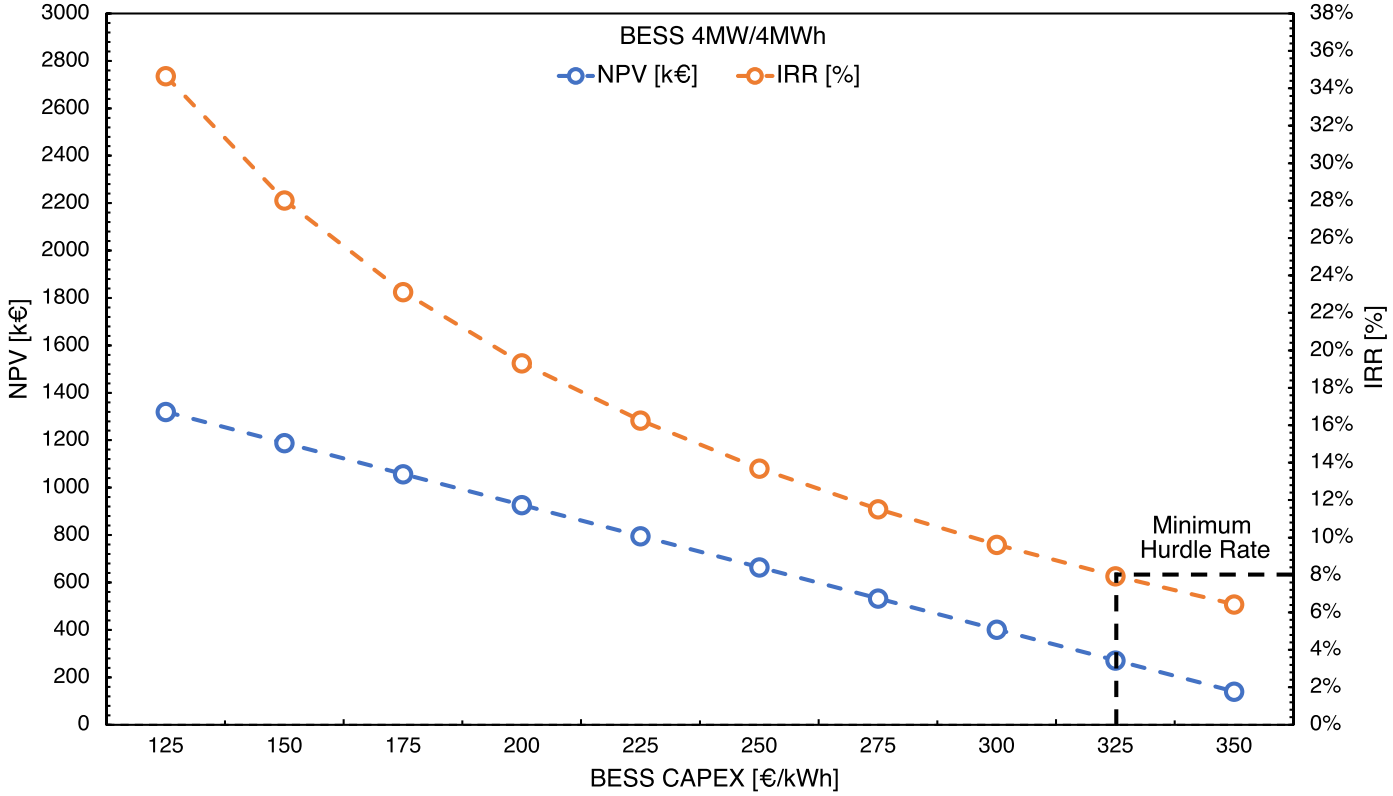

Fig. 13. NPV and IRR of the BESS investment as a function of different BESS CAPEX.

Table 11
Tabular representation of results illustrated in Fig. 13.

BESS CAPEX [€/kWh]	125	150	175	200	250	275	300	325	350
NPV [k€]	1320.10	1188.96	1057.82	926.68	795.54	664.40	533.27	402.13	270.99
IRR [%]	34.67	28.02	23.13	19.33	16.25	13.70	11.52	9.62	7.94

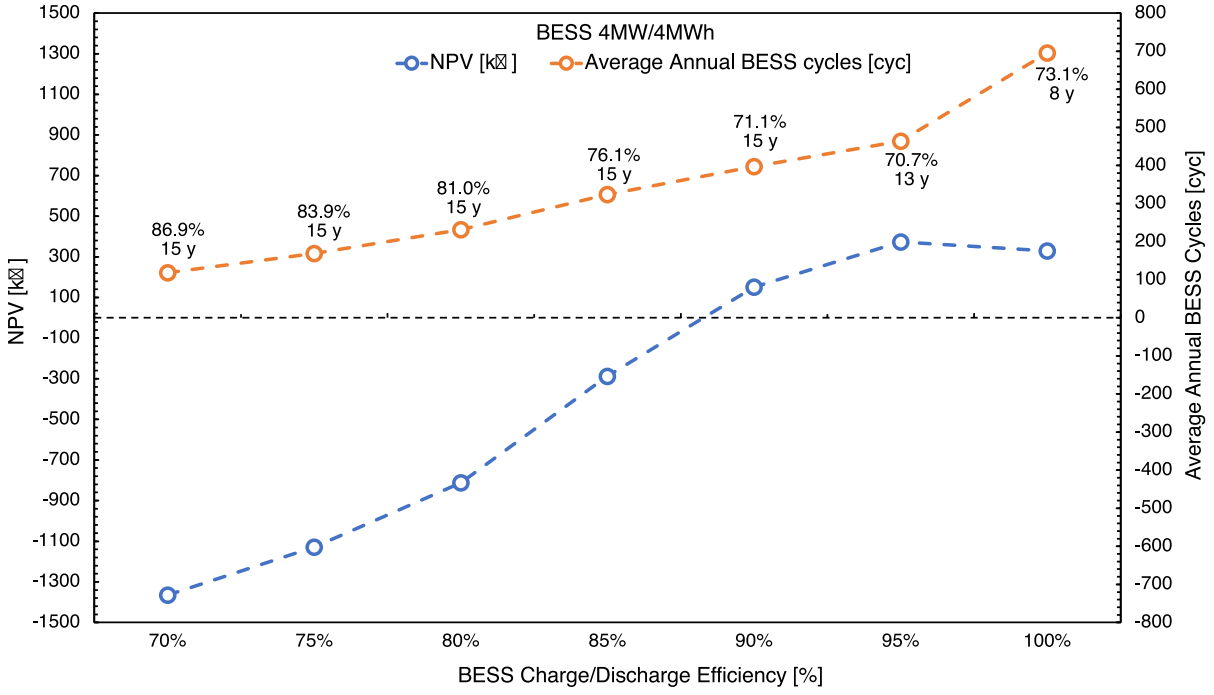

Fig. 14. NPV of the BESS investment and average annual BESS cycles as a function of different BESS charge/discharge efficiency values. The data labels represent the remaining capacity of the battery and the number of years to reach its end-of-life.

pronounced at lower battery costs: a reduction in battery cost from 125 €/kWh to 150 €/kWh results in a 6.6 % decrease in IRR, while a reduction from 325 €/kWh to 350 €/kWh results in only a 1.5 % decrease. The quasi-linear relationship between battery cost and NPV and IRR observed in this study aligns with the findings presented in [40], where a techno-economic model of a BESS for utilizing curtailed wind energy to supply grid-level peak demand in the UK was developed.

4.3.2. *Battery efficiency*

A sensitivity analysis of battery efficiency is performed with the BESS (size of 4 MW / 4 MWh), and all other model parameters are held constant. The results of this sensitivity analysis are presented in Fig. 14, which illustrates the impact of battery charge and discharge efficiencies on both the net present value (NPV) and the average annual BESS cycles. The NPV, represented by the blue curve, corresponds to the left axis, while the orange curve represents the average annual BESS number of cycles, and it refers to the right axis. These economic and energy indicators are plotted as a function of different charge/discharge efficiency values, ranging from 70 % to 100 %, in 5 % increments. As reported in Table 2, the proposed case study discussed in Section 4.1 and in Section 4.2 considered a battery charge/discharge efficiency of 90 %, corresponding to a round-trip value of approximately 81 %.

The results reveal a clear relationship between BESS efficiency and its techno-economic performance. As BESS efficiency increases from 70 % to 100 %, the NPV shifts significantly from negative to positive values, underscoring the financial viability associated with higher efficiency levels. Specifically, the analysis shows that if the charge/discharge efficiency drops below approximately 88–89 %, our simulations predict a negative NPV, indicating that the system would not be financially viable under such conditions. This finding underscores the critical importance of maintaining high battery efficiencies to ensure the profitability of the BESS. The results align with existing literature, which reports Li-ion battery efficiencies ranging from 85 % to 98 % [67], suggesting that battery technology advancements could further enhance energy storage systems' economic returns. As the efficiency increases from 90 % to 95 %, the NPV rises from approximately 152 k€ to 373 k€, representing an increase of 222 k€.

Similarly, as BESS efficiency increases from 70 % to 100 %, the average annual cycles of the battery also increase, reflecting higher utilization of the available energy within the battery. The term "average annual cycles" refers to the average number of cycles completed yearly over the entire BESS lifetime until the end-of-life (EOL) criterion is reached. The average number of cycles increases from approximately 118 cycles per year at 70 % efficiency to about 696 cycles per year at 100 % efficiency. However, the maximum NPV value is achieved for a 95 % charge/discharge efficiency. The text in black explains this outcome in the figure, which indicates the battery's remaining capacity, and the number of years required to reach its EOL. Higher battery utilization leads to faster attainment of the EOL criterion. For example, with 100 % efficiency and an average of 696 cycles per year, the EOL is reached after just 8 years. In contrast, at 95 % efficiency and approximately 464 cycles per year, the EOL is reached after 13 years. Consequently, the NPV is higher in the 95 % efficiency scenario than the 100 % efficiency scenario because it is evaluated over a more extended period (13 years). A tabular representation of the NPV and average annual BESS cycles at different efficiency values is reported in Table 12.

A similar pattern was observed in [40], where the battery charge/discharge efficiencies varied from 75 % to 100 %. In that study, negative NPV values were predicted when the efficiencies dropped below 83 %, whereas in our work, negative NPV values are observed when the

Table 12
Tabular representation of results illustrated in Fig. 14.

BESS charge/discharge efficiency [%]	70	75	80	85	90	95	100
NPV [k€]	−1364.69	−1128.99	−812.60	−287.49	151.72	373.31	329.18
Average annual BESS cycles [cyc]	118.44	168.68	231.38	323.53	397.33	463.96	695.75

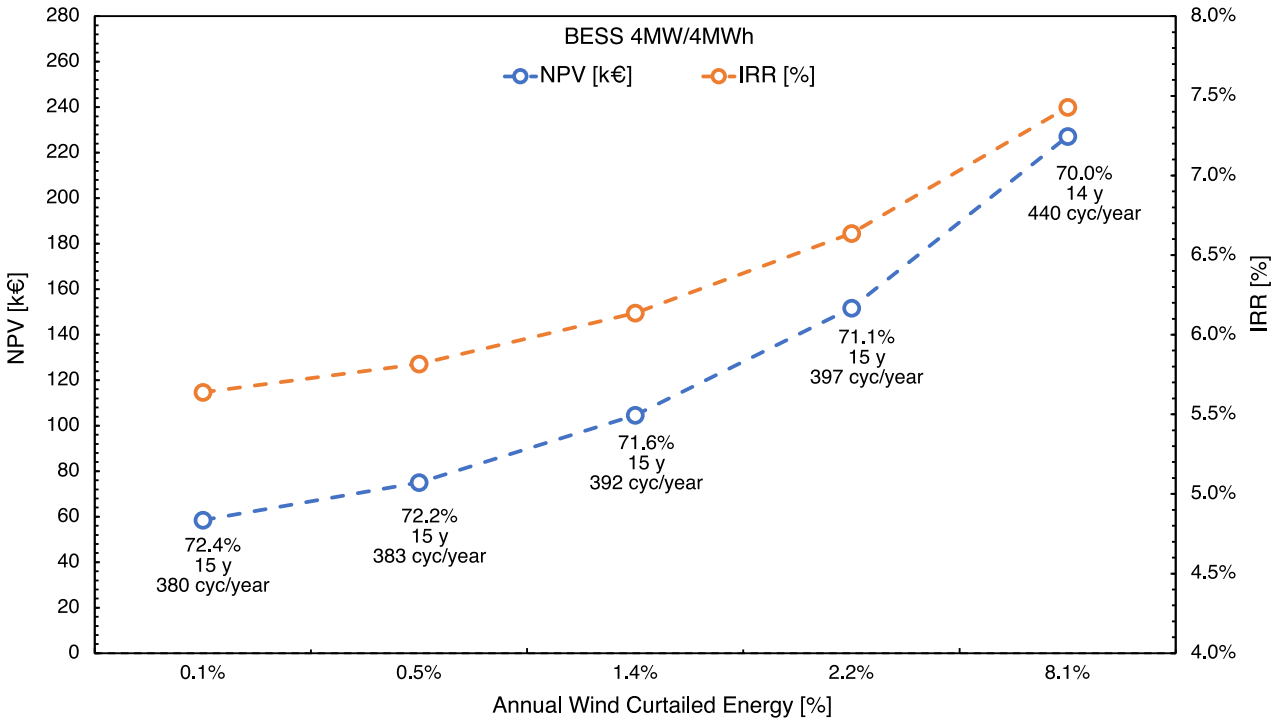

Fig. 15. NPV and IRR of the BESS investment as a function of different annual wind curtailed energy share. The text in black represents the remaining capacity of the battery, the number of years to reach its end-of-life, and the average annual number of cycles.

charge/discharge efficiency decreases below approximately 88–89 %. Unlike our results, which show a maximum NPV value at a charge/discharge efficiency of 95 %, the findings in [40] indicate a linear relationship between NPV and BESS charge/discharge efficiency. This divergence can be attributed to differences in the NPV evaluation periods: in our simulations, the NPV at 100 % charge/discharge efficiency is calculated over 8 years, reflecting the time required to reach the end-of-life (EOL) criterion. In contrast, authors in [40] assume a constant BESS lifetime of 15 years.

4.3.3. *Wind curtailed energy*

The plot presented in Fig. 15 illustrates the impact of varying annual wind curtailed energy levels on both the net present value (NPV) and the internal rate of return (IRR), considering the BESS size of 4 MW / 4 MWh. All other model parameters were kept constant. The NPV, represented by the blue curve, corresponds to the left axis, while the IRR is represented by the orange curve and refers to the right axis. Based on the available hourly dispatching orders data sent by the transmission system operator (TSO) operating in the Italian wholesale energy market, five different wind curtailed energy scenarios are simulated. As reported in Table 2, the proposed case study considered a wind farm curtailed energy of approximately 2.2 % per year.

As the percentage of annual wind-curtailed energy increases, both NPV and IRR exhibit positive trends, reflecting the enhanced financial performance of the BESS system. Specifically, the NPV increases steadily from approximately 58 k€ at 0.1 % annual curtailed wind energy to around 227 k€ at 8.1 %. Correspondingly, the IRR also shows an upward trend, rising from about 5.6 % to 7.4 % over the same range of curtailed energy. The plot further indicates that, with an increase in wind curtailment from 1.4 % to 8.1 %, the NPV grows by approximately 123 k€, and the IRR improves by about 1.3 %. This outcome highlights the direct relationship between the extent of wind curtailment and the financial viability of the BESS. Additionally, these results are consistent with the notion that greater wind curtailment leads to more opportunities for the BESS to store excess energy, thereby improving its utilization and economic returns. In fact, the higher BESS utilization resulting from increased wind curtailment leads to a higher amount of energy discharged back into the grid, particularly during periods of high energy prices (peak periods). As a result, the revenue from energy arbitrage is significantly increased. This finding is further demonstrated by the text in black on the plot, which notes the number of cycles per year and the corresponding duration to reach the EOL criterion. Accordingly, at 8.1 % annual wind curtailed energy, the BESS is projected to undergo approximately 440 cycles per year and reach its EOL in 14 years. Conversely, at 0.1 % annual wind curtailed energy, the opportunities for the battery to store excess energy are significantly reduced, in fact it is projected to undergo approximately 380 cycles per year and reach 72.4 % of remaining capacity after 15 years of operations. A tabular representation of the NPV and IRR values at different annual wind curtailed energy shares is reported in Table 13.

Table 13
Tabular representation of results illustrated in Fig. 15.

Annual wind curtailed energy [%]	0.1	0.5	1.4	2.2	8.1
NPV [k€]	58.44	75.00	104.60	151.72	227.12
IRR [%]	5.64	5.82	6.14	6.64	7.43

The trend observed in this sensitivity analysis of wind curtailed energy is consistent with the findings presented in [40]. Specifically, in that study, the amount of daily wind curtailed energy was varied between 5 % and 25 % in increments of 5 %. The results demonstrated that both the NPV and IRR increase at a higher rate as the level of wind curtailment rises. For instance, a 1 % increase in wind curtailment beyond 15 % led to an increase in NPV by £4 million and an improvement in IRR by 0.1 %.

Overall, this sensitivity analysis underscores the critical role of wind curtailment in determining the optimal performance and economic returns of a BESS. The findings suggest that the BESS becomes more financially viable as wind curtailment increases, with a higher NPV and IRR. This insight is essential for optimizing the integration of BESS into wind energy systems, particularly in regions where wind curtailment is prevalent.

5. Conclusion and future work

This work comprehensively analyzes the techno-economic viability of integrating a battery energy storage system (BESS) with an existing wind farm for grid-level wholesale energy arbitrage, particularly considering wind curtailment and battery degradation. By developing and implementing a mixed-integer linear programming (MILP) optimization model, we have identified the optimal BESS size and scheduling operations that maximize the net present value (NPV) of such system in the Italian electricity market. This approach offers a robust and replicable methodology that can be adapted for similar applications in other regions and market conditions. Additionally, by adjusting the descriptive parameters of the storage technology, different solutions can be easily evaluated and compared with one another.

Our findings demonstrate that comparing different sizes of the BESS in terms of power and capacity, the highest economic benefit is achieved by integrating a 1-h and 2-h battery into the existing wind farm. The highest NPV of 152 k€ is achieved with a 1-h BESS of 4 MW / 4 MWh. For a 2-h configuration, the highest NPV of 142 k€ is reached with a BESS size of 2 MW / 4 MWh. This result is particularly relevant given the increasing interest in renewable energy integration and the critical role that energy storage systems play in enhancing the reliability and profitability of renewable energy projects. The study also shows that the optimal scheduling of the wind-BESS system is crucial for maximizing economic returns, highlighting the importance of advanced energy management strategies that can effectively respond to market signals and operational constraints.

The sensitivity analyses conducted as part of this study highlighted the critical role of key factors such as battery costs, efficiency, and wind curtailment on the profitability of the BESS investment. Specifically, we found that battery costs need to be reduced to below 325 €/kWh for the BESS integration project under investigation to be financially viable. This finding underscores the importance of ongoing advancements in battery manufacturing and economies of scale, which are essential for making energy storage more accessible and economically feasible. Additionally, maintaining high charge/discharge efficiencies was shown to be essential to achieving a positive NPV, with our simulations indicating that efficiencies below approximately 88–89 % would result in negative profitability, making the system financially unviable. This emphasizes the importance of battery efficiency improvements through technological advancements and optimized operational strategies. While these findings demonstrate the promising potential of integrating BESS into wind farms, it is also essential to recognize the existing limitations related to profitability. These limitations, primarily driven by the high costs of batteries and their efficiencies, were particularly evident in the sensitivity analyses. This balanced view underscores that, despite the positive prospects, the financial viability of BESS remains closely tied to overcoming these challenges, which future technological advancements must address.

Moreover, incorporating a cycle-counting degradation model within the optimization framework proved crucial for obtaining realistic profitability assessments. This model accurately accounted for the effects of battery ageing, which directly impacts the system's economic returns over its operational lifetime. Without considering battery degradation, profitability evaluations could be overly optimistic, potentially leading to misguided investment decisions. Our analysis revealed that as the battery degrades, both the capacity and the annual net profit gradually decrease, underscoring the need for careful consideration of degradation in long-term financial projections. This also suggests that policies and incentives aimed at promoting battery storage should consider the long-term degradation effects to ensure that investments remain viable over the entire project lifecycle.

The research also highlights the importance of considering wind curtailment as a further opportunity for energy storage to directly enhance financial performance. The results indicate that higher levels of wind curtailment allow the BESS to store more excess energy, thereby improving its utilization and leading to higher NPV and internal rate of return (IRR). This relationship highlights the potential for BESS to mitigate the negative impacts of wind curtailment, making renewable energy systems more efficient and economically viable. This is particularly important in regions where grid congestion or limited transmission capacity leads to significant wind energy curtailment.

While this study offers valuable insights into the long-term profitability of integrating a utility-scale BESS with an existing wind farm, certain limitations should be acknowledged, and avenues for future work should be highlighted. Firstly, the proposed method assumes perfect foresight of wholesale energy prices and dispatching orders, which may not fully capture the uncertainty inherent in real-world operations. Incorporating stochastic optimization frameworks or robust decision-making approaches could enhance the reliability of the results, particularly in markets with high price volatility. Furthermore, the degradation model employed in this work is based on linear approximations, which, while computationally efficient, may oversimplify the impact of factors such as cycle depth and temperature variations. Developing more detailed, non-linear degradation models would improve the accuracy of long-term performance and profitability estimates. Another limitation of this study lies in its focus on energy arbitrage and wind curtailment mitigation. While these applications are fundamental in existent and future power grids, future work could expand the scope to include ancillary services such as frequency regulation, operating reserves, and demand response. Co-optimizing these services alongside energy arbitrage could uncover synergies and trade-offs that inform more comprehensive operational strategies. Additionally, this research does not consider hybrid storage solutions or emerging battery technologies that may provide enhanced performance or cost benefits. Exploring these technologies could unlock new opportunities for optimization. Lastly, while this study focuses on the Italian electricity market, the findings may not fully generalize to other regions with differing market structures and regulatory environments. Extending the analysis to other geographic contexts and examining the influence of evolving policies, such as carbon pricing and renewable incentives, would provide a broader perspective on the economic viability of BESS integration. Experimental validation through field trials or laboratory-scale implementations could also strengthen the findings and provide practical feedback for refining the proposed methodology. By addressing these limitations and exploring these future directions, the integration of utility-scale BESS with renewable energy systems can be further optimized, contributing to a more sustainable and resilient energy future.

CRediT authorship contribution statement

Alberto Grimaldi: Writing – original draft, Visualization, Software, Methodology, Investigation, Formal analysis, Data curation, Conceptualization. **Francesco Demetrio Minuto:** Writing – review & editing, Methodology, Investigation, Conceptualization. **Alessandro Perol:**

Writing – review & editing, Conceptualization. **Silvia Casagrande:** Writing – review & editing, Conceptualization. **Andrea Lanzini:** Writing – review & editing, Supervision, Conceptualization.

Declaration of competing interest

The authors declare the following financial interests/personal relationships which may be considered as potential competing interests: Francesco Demetrio Minuto reports financial support was provided by FSE REACT-EU - PON Ricerca e Innovazione 2014–2020. If there are other authors, they declare that they have no known competing financial interests or personal relationships that could have appeared to influence the work reported in this paper.

Acknowledgements

Francesco Demetrio Minuto carried out this study within the Ministerial Decree no. 1062/2021 and received funding from the FSE REACT-EU - PON Ricerca e Innovazione 2014-2020. This manuscript reflects only the authors' views and opinions, neither the European Union nor the European Commission can be considered responsible for them. The authors would like to thank Bachisio Solinas, a master's degree student at Politecnico di Torino University, for his contribution to this research as part of his master's thesis project.

Data availability

The data that has been used is confidential.

References

[1] International Energy Agency, World Energy Outlook Special Report Batteries and Secure Energy Transitions, IEA, Paris, 2023.
[2] Bloomberg New Energy Finance (BNEF), 2H 2023 Energy Storage Market Outlook, Policies Translating to Projects, 2023. https://about.bnef.com/blog/2h-2023-energy-storage-market-outlook/ (accessed May 27, 2024).
[3] R. Novo, F.D. Minuto, G. Bracco, G. Mattiazzo, R. Borchiellini, A. Lanzini, Supporting Decarbonization strategies of local energy systems by De-risking Investments in Renewables: a case study on Pantelleria Island, Energies (Basel) 15 (2022), https://doi.org/10.3390/en15031103.
[4] F. Mohamad, J. Teh, C.M. Lai, L.R. Chen, Development of energy storage systems for power network reliability: a review, Energies (Basel) 11 (2018), https://doi.org/10.3390/en11092278.
[5] I. Staffell, M. Rustomji, Maximising the value of electricity storage, J Energy Storage 8 (2016) 212–225, https://doi.org/10.1016/j.est.2016.08.010.
[6] I.N. Moghaddam, B. Chowdhury, M. Doostan, Optimal sizing and operation of battery energy storage systems connected to wind farms participating in electricity markets, IEEE Trans Sustain Energy 10 (2019) 1184–1193, https://doi.org/10.1109/TSTE.2018.2863272.
[7] L.M.S. de Siqueira, W. Peng, Control strategy to smooth wind power output using battery energy storage system: a review, J Energy Storage 35 (2021), https://doi.org/10.1016/j.est.2021.102252.
[8] G. He, Q. Chen, C. Kang, P. Pinson, Q. Xia, Optimal bidding strategy of battery storage in power markets considering performance-based regulation and battery cycle life, IEEE Trans Smart Grid 7 (2016) 2359–2367, https://doi.org/10.1109/TSG.2015.2424314.
[9] H. Mohsenian-Rad, Optimal bidding, scheduling, and deployment of battery systems in California day-ahead energy market, IEEE Trans. Power Syst. 31 (2016) 442–453, https://doi.org/10.1109/TPWRS.2015.2394355.
[10] M. Kazemi, H. Zareipour, Long-term scheduling of battery storage systems in energy and regulation markets considering battery's lifespan, IEEE Trans Smart Grid 9 (2018) 6840–6849, https://doi.org/10.1109/TSG.2017.2724919.
[11] Y. Shi, B. Xu, D. Wang, B. Zhang, Using battery storage for peak shaving and frequency regulation: joint Optimization for Superlinear gains, IEEE Trans. Power Syst. 33 (2018) 2882–2894, https://doi.org/10.1109/TPWRS.2017.2749512.
[12] B. Xu, J. Zhao, T. Zheng, E. Litvinov, D.S. Kirschen, Factoring the cycle aging cost of batteries participating in electricity markets, IEEE Trans. Power Syst. 33 (2018) 2248–2259, https://doi.org/10.1109/TPWRS.2017.2733339.
[13] G. He, S. Kar, J. Mohammadi, P. Moutis, J.F. Whitacre, Power system dispatch with marginal degradation cost of battery storage, IEEE Trans. Power Syst. 36 (2021) 3552–3562, https://doi.org/10.1109/TPWRS.2020.3048401.
[14] S. Shafiee, P. Zamani-Dehkordi, H. Zareipour, A.M. Knight, Economic assessment of a price-maker energy storage facility in the Alberta electricity market, Energy 111 (2016) 537–547, https://doi.org/10.1016/j.energy.2016.05.086.
[15] E. Nasrolahpour, J. Kazempour, H. Zareipour, W.D. Rosehart, A Bilevel model for participation of a storage system in energy and reserve markets, IEEE Trans Sustain Energy 9 (2018) 582–598, https://doi.org/10.1109/TSTE.2017.2749434.
[16] H. Mohsenian-Rad, Coordinated Price-maker operation of large energy storage units in nodal energy markets, IEEE Trans. Power Syst. 31 (2016) 786–797, https://doi.org/10.1109/TPWRS.2015.2411556.
[17] H. Ding, P. Pinson, Z. Hu, J. Wang, Y. Song, Optimal offering and operating strategy for a large wind-storage system as a Price maker, IEEE Trans. Power Syst. 32 (2017) 4904–4913, https://doi.org/10.1109/TPWRS.2017.2681720.
[18] H. Cui, F. Li, X. Fang, H. Chen, H. Wang, Bilevel arbitrage potential evaluation for grid-scale energy storage considering wind power and LMP smoothing effect, IEEE Trans Sustain Energy 9 (2018) 707–718, https://doi.org/10.1109/TSTE.2017.2758378.
[19] J.F. Toubeau, J. Bottieau, Z. De Greeve, F. Vallee, K. Bruninx, Data-driven scheduling of energy storage in day-ahead energy and reserve markets with probabilistic guarantees on real-time delivery, IEEE Trans. Power Syst. 36 (2021) 2815–2828, https://doi.org/10.1109/TPWRS.2020.3046710.
[20] J. Arteaga, H. Zareipour, A Price-maker/Price-taker model for the operation of battery storage systems in electricity markets, IEEE Trans Smart Grid 10 (2019) 6912–6920, https://doi.org/10.1109/TSG.2019.2913818.
[21] A.V. Vykhodtsev, D. Jang, Q. Wang, W. Rosehart, H. Zareipour, A review of modelling approaches to characterize lithium-ion battery energy storage systems in techno-economic analyses of power systems, Renew. Sust. Energ. Rev. 166 (2022), https://doi.org/10.1016/j.rser.2022.112584.
[22] Y. Yang, S. Bremner, C. Menictas, M. Kay, Modelling and optimal energy management for battery energy storage systems in renewable energy systems: a review, Renew. Sust. Energ. Rev. 167 (2022), https://doi.org/10.1016/j.rser.2022.112671.
[23] N. Collath, B. Tepe, S. Englberger, A. Jossen, H. Hesse, Aging aware operation of lithium-ion battery energy storage systems: a review, J Energy Storage 55 (2022), https://doi.org/10.14459/2022m.
[24] B. Xu, A. Oudalov, A. Ulbig, G. Andersson, D.S. Kirschen, Modeling of lithium-ion battery degradation for cell life assessment, IEEE Trans Smart Grid 9 (2018) 1131–1140, https://doi.org/10.1109/TSG.2016.2578950.
[25] B. Zakeri, S. Syri, Electrical energy storage systems: a comparative life cycle cost analysis, Renew. Sust. Energ. Rev. 42 (2015) 569–596, https://doi.org/10.1016/j.rser.2014.10.011.
[26] A. Nuhic, T. Terzimehic, T. Soczka-Guth, M. Buchholz, K. Dietmayer, Health diagnosis and remaining useful life prognostics of lithium-ion batteries using data-driven methods, J. Power Sources 239 (2013) 680–688, https://doi.org/10.1016/j.jpowsour.2012.11.146.
[27] P. Marques, R. Garcia, L. Kulay, F. Freire, Comparative life cycle assessment of lithium-ion batteries for electric vehicles addressing capacity fade, J. Clean. Prod. 229 (2019) 787–794, https://doi.org/10.1016/j.jclepro.2019.05.026.
[28] Á. Arcos-Vargas, D. Canca, F. Núñez, Impact of battery technological progress on electricity arbitrage: an application to the Iberian market, Appl. Energy 260 (2020), https://doi.org/10.1016/j.apenergy.2019.114273.
[29] A. Maheshwari, N.G. Paterakis, M. Santarelli, M. Gibescu, Optimizing the operation of energy storage using a non-linear lithium-ion battery degradation model, Appl. Energy 261 (2020), https://doi.org/10.1016/j.apenergy.2019.114360.
[30] R.L. Fares, M.E. Webber, What are the tradeoffs between battery energy storage cycle life and calendar life in the energy arbitrage application? J Energy Storage 16 (2018) 37–45, https://doi.org/10.1016/j.est.2018.01.002.
[31] G. He, Q. Chen, P. Moutis, S. Kar, J.F. Whitacre, An intertemporal decision framework for electrochemical energy storage management, Nat. Energy 3 (2018) 404–412, https://doi.org/10.1038/s41560-018-0129-9.
[32] F. Wankmüller, P.R. Thimmapuram, K.G. Gallagher, A. Botterud, Impact of battery degradation on energy arbitrage revenue of grid-level energy storage, J Energy Storage 10 (2017) 56–66, https://doi.org/10.1016/j.est.2016.12.004.
[33] A. Grimaldi, F.D. Minuto, A. Perol, S. Casagrande, A. Lanzini, Ageing and energy performance analysis of a utility-scale lithium-ion battery for power grid applications through a data-driven empirical modelling approach, J Energy Storage 65 (2023), https://doi.org/10.1016/j.est.2023.107232.
[34] S. Li, H. He, C. Su, P. Zhao, Data driven battery modeling and management method with aging phenomenon considered, Appl. Energy 275 (2020), https://doi.org/10.1016/j.apenergy.2020.115340.
[35] B. Xu, Y. Shi, D.S. Kirschen, B. Zhang, Optimal battery participation in frequency regulation markets, IEEE Trans. Power Syst. 33 (2018) 6715–6725, https://doi.org/10.1109/TPWRS.2018.2846774.
[36] M. Miletić, H. Pandžić, D. Yang, Operating and investment models for energy storage systems, Energies (Basel) 13 (2020), https://doi.org/10.3390/en13184600.
[37] M.A. Hannan, S.B. Wali, P.J. Ker, M.S.A. Rahman, M. Mansor, V. K. Ramachandaramurthy, K.M. Muttaqi, T.M.I. Mahlia, Z.Y. Dong, Battery energy-storage system: a review of technologies, optimization objectives, constraints, approaches, and outstanding issues, J Energy Storage 42 (2021), https://doi.org/10.1016/j.est.2021.103023.
[38] N. Padmanabhan, M. Ahmed, K. Bhattacharya, Battery energy storage Systems in Energy and Reserve Markets, IEEE Trans. Power Syst. 35 (2020) 215–226, https://doi.org/10.1109/TPWRS.2019.2936131.
[39] A. Perez, R. Moreno, R. Moreira, M. Orchard, G. Strbac, Effect of battery degradation on multi-service portfolios of energy storage, IEEE Trans Sustain Energy 7 (2016) 1718–1729, https://doi.org/10.1109/TSTE.2016.2589943.
[40] N.S. Rayit, J.I. Chowdhury, N. Balta-Ozkan, Techno-economic optimisation of battery storage for grid-level energy services using curtailed energy from wind, J Energy Storage 39 (2021), https://doi.org/10.1016/j.est.2021.102641.
[41] C. Sheridan, M. Conlon, A techno-economic evaluation of battery energy storage systems co-located with wind in the Irish integrated electricity market, in: In: 2021 56th International Universities Power Engineering Conference: Powering Net Zero

Emissions, UPEC 2021 - Proceedings, Institute of Electrical and Electronics Engineers Inc., 2021, https://doi.org/10.1109/UPEC50034.2021.9548207.
[42] L. Feng, X. Zhang, C. Li, X. Li, B. Li, J. Ding, C. Zhang, H. Qiu, Y. Xu, H. Chen, Optimization analysis of energy storage application based on electricity price arbitrage and ancillary services, J Energy Storage 55 (2022), https://doi.org/10.1016/j.est.2022.105508.
[43] E. Lobato, L. Sigrist, A. Ortega, A. González, J.M. Fernández, Battery energy storage integration in wind farms: economic viability in the Spanish market, sustainable energy, Grids and Networks 32 (2022), https://doi.org/10.1016/j.segan.2022.100854.
[44] D. Cremoncini, G.F. Frate, A. Bischi, T.T. Pedersen, G.B. Andresen, A. Bentien, L. Ferrari, Optimal participation of a wind and hybrid battery storage system in the day-ahead and automatic frequency restoration reserve markets, J Energy Storage 94 (2024), https://doi.org/10.1016/j.est.2024.112309.
[45] M. Dicorato, G. Forte, M. Pisani, M. Trovato, Planning and operating combined wind-storage system in electricity market, IEEE Trans Sustain Energy 3 (2012) 209–217, https://doi.org/10.1109/TSTE.2011.2179953.
[46] J. Li, C. Wang, H. Wang, Optimal energy storage scheduling for wind curtailment reduction and energy arbitrage: A deep reinforcement learning approach, in: IEEE Power and Energy Society General Meeting, IEEE Computer Society, 2023, https://doi.org/10.1109/PESGM52003.2023.10253181.
[47] M. Khalid, R.P. Aguilera, A.V. Savkin, V.G. Agelidis, On maximizing profit of wind-battery supported power station based on wind power and energy price forecasting, Appl. Energy 211 (2018) 764–773, https://doi.org/10.1016/j.apenergy.2017.11.061.
[48] O. Schmidt, I. Staffell, Monetizing energy storage – a toolkit to assess future cost and value, Oxford University Press (2023), https://doi.org/10.1093/oso/9780192888174.001.0001.
[49] T.Y. Lee, Operating schedule of battery energy storage system in a time-of-use rate industrial user with wind turbine generators: a multipass iteration particle swarm optimization approach, IEEE Transactions on Energy Conversion 22 (2007) 774–782, https://doi.org/10.1109/TEC.2006.878239.
[50] L. Joerissen, J. Garche, C. Fabjan, G. Tomazic, Possible use of vanadium redox-flow batteries for energy storage in small grids and stand-alone photovoltaic systems, J. Power Sources (2004) 98–104, https://doi.org/10.1016/j.jpowsour.2003.09.066.
[51] Z. Liu, Z. Zhang, R. Zhuo, X. Wang, Optimal operation of independent regional power grid with multiple wind-solar-hydro-battery power, Appl. Energy 235 (2019) 1541–1550, https://doi.org/10.1016/j.apenergy.2018.11.072.
[52] J. Hossain, N. Saeed, R. Manojkumar, M. Marzband, K. Sedraoui, Y. Al-Turki, Optimal peak-shaving for dynamic demand response in smart Malaysian commercial buildings utilizing an efficient PV-BES system, Sustain. Cities Soc. 101 (2024), https://doi.org/10.1016/j.scs.2023.105107.
[53] M. Gupta, Market Report Solar-Plus-Storage System Architectures: Design, Pricing and Economics in the US, Tech. Rep.,, Wood Mackenzie Power & Renewables, 2019.
[54] GME - Gestore dei Mercati Energetici SpA, Esiti dei mercati e statistiche - Statistiche - Dati storici Excel, (2024). https://www.mercatoelettrico.org/it/ (accessed June 7, 2024).
[55] N. DiOrio, P. Denholm, W.B. Hobbs, A model for evaluating the configuration and dispatch of PV plus battery power plants, Appl. Energy 262 (2020), https://doi.org/10.1016/j.apenergy.2019.114465.
[56] A. Grimaldi, F.D. Minuto, J. Brouwer, A. Lanzini, Profitability of energy arbitrage net profit for grid-scale battery energy storage considering dynamic efficiency and degradation using a linear, mixed-integer linear, and mixed-integer non-linear optimization approach, J Energy Storage 95 (2024) 112380, https://doi.org/10.1016/j.est.2024.112380.
[57] M. L. Bynum, G. A. Hackebeil, W. E. Hart, C. D. Laird, B. L. Nicholson, J. D. Siirola, J. Watson, D. L. Woodruff, Pyomo – Optimization Modeling in Python Third Edition, Springer Optimization and Its Applications, Vol. 67, 2021. http://www.springer.com/series/7393.
[58] L.L.C. Gurobi Optimization, Gurobi optimizer reference manual. https://www.gurobi.com, 2022. (Accessed 28 April 2023).
[59] D. Kumar, Reinforcement learning for energy storage arbitrage in the day-ahead and real-time markets with accurate Li-ion battery dynamics model, Master Thesis of Engineering in Electrical Engineering and Computer Science at the Massachusetts Institute of Technology (2021) 29. https://hdl.handle.net/1721.1/139292. (Accessed 14 October 2024).
[60] I. Pavić, N. Čović, H. Pandžić, PV–battery-hydrogen plant: cutting green hydrogen costs through multi-market positioning, Appl. Energy 328 (2022), https://doi.org/10.1016/j.apenergy.2022.120103.
[61] H.C. Hesse, V. Kumtepeli, M. Schimpe, J. Reniers, D.A. Howey, A. Tripathi, Y. Wang, A. Jossen, Ageing and efficiency aware battery dispatch for arbitrage markets using mixed integer linear programming, Energies (Basel) 12 (2019), https://doi.org/10.3390/en12060999.
[62] M. Cococcioni, L. Fiaschi, The big-M method with the numerical infinite M, Optim. Lett. 15 (2021) 2455–2468, https://doi.org/10.1007/s11590-020-01644-6.
[63] O. Schmidt, S. Melchior, A. Hawkes, I. Staffell, Projecting the future Levelized cost of electricity storage technologies, Joule 3 (2019) 81–100, https://doi.org/10.1016/j.joule.2018.12.008.
[64] World Energy Council, E-Storage: Shifting Cost to Value Wind and Solar Applications, Used by Permission of the World Energy Council, London, www.worldenergy.org, 2016.
[65] F. Judge, F.D. McAuliffe, I.B. Sperstad, R. Chester, B. Flannery, K. Lynch, J. Murphy, A lifecycle financial analysis model for offshore wind farms, Renew. Sust. Energ. Rev. 103 (2019) 370–383, https://doi.org/10.1016/j.rser.2018.12.045.
[66] C. Augustine, N. Blair, Storage Futures Study: Storage Technology Modeling Input Data Report, Golden, National Renewable Energy Laboratory, CO, 2021. https://www.nrel.gov/docs/fy21osti/78694.pdf.
[67] S. Koohi-Fayegh, M.A. Rosen, A review of energy storage types, applications and recent developments, J Energy Storage 27 (2020), https://doi.org/10.1016/j.est.2019.101047.
[68] U.K. Exchange Rates, Compare Live Foreign Currency Exchange Rate & History. https://www.exchangerates.org.uk/, 2024. (Accessed 14 October 2024).